Maternal Dead-end 1 Promotes Translation of *nanos1* Through Binding the eIF3 Complex

Tristan Aguero[1,#], Zhigang Jin[2,#], Sandip Chorghade[3], Auinash Kalsotra[3], Mary Lou King[1,§] and Jing Yang[2,4,§]

[1]Department of Cell Biology, University of Miami, Miami, FL 33136, USA.

[2]Department of Comparative Biosciences, University of Illinois at Urbana-Champaign, IL 61802, USA.

[3]Department of Biochemistry, University of Illinois at Urbana-Champaign, Urbana, IL 61801, USA.

[4]Lead contact

# contributed equally

[§]To whom correspondence should be addressed.

Co-corresponding authors:

Mary Lou King (MKing@med.miami.edu)

Jing Yang (yangj@illinois.edu)

Keywords: germline development, translation regulation, Dnd1, Nanos, *Xenopus*

Abstract: In the developing embryo, primordial germ cells (PGCs) represent the exclusive progenitors of the gametes, and their loss results in adult infertility. During early development, PGCs are exposed to numerous signals that specify somatic cell fates. To prevent somatic differentiation, PGCs must transiently silence their genome, an early developmental process that requires Nanos activity. However, it is unclear how *nanos* translation is regulated in developing embryos. We report here that translation of *nanos1* after fertilization requires Dead End1 (Dnd1), a vertebrate-specific germline RNA-binding protein. We provide evidence that Dnd1 protein, whose expression is low in oocytes, but increases dramatically after fertilization, directly interacts with, and relieves the inhibitory function of eukaryotic initiation factor 3f, a repressive component in the 43S preinitiation complex. This work uncovers a novel translational regulatory mechanism that is fundamentally important for germline development.

Summary Statement

Nanos proteins prevent somatic differentiation of primordial germ cells. We show that Dead End1 (Dnd1) binds *nanos1* mRNA and promotes *nanos1* translation by directly interacting with the translational machinery.

Introduction

Primordial germ cells (PGCs), considered the "stem cells of the species" (Wylie, 1999), can be specified through inheritance of germ plasm or embryonic induction (Extavour and Akam, 2003; Saitou, 2009; Strome and Lehmann, 2007). Despite the differences in how PGCs are specified, after specification, many aspects of PGC development are highly conserved. In all species, the totipotent potential of the newly specified PGCs is protected by multiple mechanisms including: global transcriptional repression, DNA methylation, chromatin alteration, and germline specific translational regulation. Interfering with these regulatory mechanisms in PGCs often results in reduction or elimination of germ cells, ultimately causing infertility (Strome and Updike, 2015).

Nanos is an evolutionarily conserved germline zinc-finger protein that plays important roles in protecting germ cell fate during early stages of PGC development (Curtis et al., 1997). In *Drosophila*, *C. elegans*, and *Xenopus*, loss of Nanos results in premature zygotic transcription, misexpression of somatic genes in the germline, and apoptosis of PGCs (Deshpande et al., 1999; Lai et al., 2012; Sato et al., 2007; Schaner et al., 2003). Nanos acts together with the RNA binding protein Pumilio (Jaruzelska et al., 2003; Nakahata et al., 2001; Sonoda and Wharton, 1999; Sonoda and Wharton, 2001) to repress translation of its target mRNAs. These include *cyclin B1* in *Drosophila* and *Xenopus* (Asaoka-Taguchi et al., 1999; Dalby and Glover, 1993; Kadyrova et al., 2007; Lai et al., 2011), *hunchback* (Murata and Wharton, 1995; Wreden et al., 1997) and *bicoid* in *Drosophila* (Wharton and Struhl, 1991), *fem-3* in *C. elegans* (Ahringer and Kimble, 1991; Zhang et al., 1997), and *VegT* in *Xenopus* (Lai et al., 2012). Proper regulation of Nanos expression is critically important for normal germline development.

In *Xenopus*, maternal *nanos1* mRNA is sequestered in an untranslated state during oogenesis (Mosquera et al., 1993; Zhou and King, 1996). Misexpression of Nanos in oocytes results in abnormal embryonic development (Luo et al., 2011). Repression of *nanos1* translation in oocytes is mediated by a translational control element (TCE) located downstream of the first AUG in *nanos1* mRNA. After fertilization (Lai et al., 2011; Luo et al., 2011), repression is released, leading to accumulation of Nanos1 protein, which prevents premature zygotic transcription in the germline (Lai et al., 2012). Currently, it is unclear how *nanos1* translation, or any other germline RNA, is activated after fertilization.

dead end1 (dnd1) is a germ plasm specific maternal RNA that was originally discovered in zebrafish, and then in other vertebrates including *Xenopus*, chick, mouse, and human (Weidinger et al., 2003). The exclusive germline expression pattern of *dnd1* suggests that it has a conserved role in germline development. Dnd family members are RNA binding proteins bearing two RNA Recognition Motifs (RRM) in their N-terminus. In zebrafish, morpholino knockdown of Dnd1 results in abnormal migration of PGCs and eventual elimination of germ cells (Weidinger et al., 2003). Similar phenomena are also observed in *Xenopus* when Dnd1 is knocked down (Horvay et al., 2006). Some published reports suggest a link between Dnd1 and the miRNA pathway. Kedde and colleagues reported that Dnd1 promotes *nanos* expression in the zebrafish germline by masking the miRNA-binding site within the *nanos* 3'UTR. Although no direct evidence is currently available, it is proposed that zebrafish Dnd1 binds to a stretch of U-rich sequences around the *miR430*-binding sites and prevents access of the microRNAs and subsequent degradation (Kedde et al., 2007). Therefore, zebrafish Dnd1 is considered a protector of RNAs targeted for degradation. Intriguingly, recent studies in the mouse male germ line reveal that

Dnd1 also interacts with the CNOT deadenylase complex to mediate mRNA decay (Suzuki et al., 2016; Yamaji et al., 2017). It appears that Dnd1 plays a multifaceted role in the vertebrate germline.

Here, we report a novel function of Dnd1 in activating germline specific translation. Depletion of maternal *dnd1* attenuated Nanos1 expression after fertilization, even though normal levels of *nanos1* mRNA were present. Overexpression of Dnd1 in *Xenopus* oocytes resulted in premature translation of *nanos1*. Furthermore, we show that Dnd1 binds *nanos1* mRNA and promotes initiation through its direct interaction with eIF3f. We provide evidence that, in the absence of Dnd1, eIF3f suppresses *nanos1* translation. Dnd1 overcomes the repressive activity of eIF3f and activate *nanos1* translation. Our findings thus uncover a novel function of Dnd1 in translation initiation acting through the eIF3 complex within the germline.

Results

Dnd1 is necessary and sufficient for *nanos1* translation

We have previously reported that translation of *nanos1* mRNA is blocked during *Xenopus* oogenesis and activated after fertilization. Mechanistically, the translational control element (TCE), a secondary RNA structure, sterically prevents ribosome scanning and translation initiation (Luo et al., 2011). After fertilization, we hypothesize that one or more activator(s) is present within the germ plasm that is capable of altering the secondary structure, thus allowing translational initiation events to proceed. Because helicases function to resolve RNA secondary structures, we hypothesized that germline specific helicases would be good candidates for potential activator(s). RNA helicases Vasa (Liang et al., 1994), Centroid (Kloc and Chan, 2007),

DeadSouth (MacArthur et al., 2000), and eIF4A (Rogers et al., 2002) were selected as well as the translation activator Dazl (Takeda et al., 2009), and the putative helicase Dnd1 (Liu and Collodi, 2010). Transcripts of these candidates were individually co-injected into stage VI oocytes with *nanos1* mRNA and the presence of Nanos1 protein was subsequently detected by Western blot analysis after immunoprecipitation (IP) with an anti-Nanos1 antibody (Luo et al., 2011). A modified *nanos1* RNA that was depleted of the TCE, *nanos1ΔTCE*, served as a positive control for *nanos1* translation. As expected, *nanos1ΔTCE* RNA promoted the highest level of translation in our assay. *dnd1* activated *nanos1* translation to levels comparable to ΔTCE (88%; n=3), while *vasa* and *deadsouth* poorly promoted translation (16% and 5% of ΔTCE, respectively; n = 3) and *centroid* and *xDazl* did not cause *nanos1* translation (Fig. 1A, B).

Previous studies have revealed a role for Dnd1 in preserving germline RNAs by blocking their miRNA-associated degradation, but not in actively promoting germline RNA translation (Kedde et al., 2007). To determine if Dnd1 can act as a translation activator through a miRNA-independent mechanism, we tested its activity in wheat germ extracts. We reasoned that while a plant based in vitro translation system would contain all the general factors required for translation, it would not include miRNAs or translation regulators specific to vertebrate PGCs. As in oocytes, *nanos1* RNA failed to translate in wheat germ extracts, consistent with our steric hindrance model for *nanos1* (Luo et al., 2011). However, similar to what we observed in oocytes, addition of purified Dnd1 protein promoted *nanos1* translation (Fig. 1C). From this result, we concluded that Dnd1 activation of *nanos1* translation does not require additional germline specific factors, but works through a generic mechanism common to both plants and animals.

To address whether Dnd1 is required for *nanos1* translation during *Xenopus* germline development, we depleted maternal *dnd1* RNA from oocytes using thioate-modified antisense oligos. The *dnd1*-depleted oocytes were used to generate embryos by host transfer procedures (Mei et al., 2013; Mir and Heasman, 2008). The efficiency of *dnd1* RNA depletion was confirmed by quantitative PCR (qPCR) (Fig. 1D). Embryos were collected at the 8 to 16-cell stage and endogenous Nanos1 protein was detected by immunofluorescence (IF) and confocal analysis (Lai et al., 2012; Luo et al., 2011). Xiwi protein was used as a marker for germ plasm (Lau et al., 2009; Wilczynska et al., 2009). As shown in Fig. 1E, 83% (n = 18) of the uninjected controls showed co-staining of Xiwi and Nanos1 protein. Of the embryos depleted of *dnd1*, only 13% had detectable Nanos1 staining (n = 15). Importantly, *nanos1* translation was rescued by re-introducing *Xenopus tropicalis dnd1* RNA, with 78% showing Nanos1 staining within the germ plasm (n = 9). qRT-PCR analysis confirmed that *nanos1* RNA was not degraded in *dnd1*-depleted embryos (Fig. 1D), providing strong evidence in support of a new function for Dnd1 in promoting *nanos1* translation rather than stability. Collectively, these results demonstrated that Dnd1 is necessary and sufficient for *nanos1* translation. In the absence of Dnd1, other germ plasm specific factors such as Vasa and DeadSouth, could not activate *nanos1* translation.

Dnd1 binds *nanos1* mRNA *in vivo* and *in vitro*

If Dnd1 activates *nanos1* translation *in vivo*, we would expect it to be present in germ plasm well before the 8-cell stage when Nanos1 is detected there by IF (Lai et al., 2012). qPCR revealed that the level of *dnd1* mRNA remained consistent prior to gastrulation (Fig. 2A). The expression of Dnd1 protein, however, is dynamically regulated. In stark contrast to Vasa, Pumilio2, and Xiwi proteins, which are expressed at relatively constant levels during the oocyte to embryo transition,

Dnd1 is present at low levels in stage VI oocytes and ovulated eggs, but is strongly expressed in fertilized eggs (Fig. 2B). In fact, detection of Dnd1 in oocytes and ovulated eggs required enrichment by IP. Dnd1 protein was barely detected in oocytes at the vegetal cortex and found only within the germ plasm of embryos by IF (Fig. 2C). Therefore, Dnd1 is present at the right time and place to regulate *nanos1* translation.

To determine if Dnd1 is capable of binding *nanos1* RNA, we used purified recombinant Dnd1 protein (Supplemental Fig. 1) and ^{32}P-labeled *nanos1* RNA and performed a quantitative double filter-binding assay. The binding curve showed that Dnd1 interacted with the *nanos1* RNA with a dissociation constant of ~140 nM (Fig. 3A). Thus, Dnd1 protein, without additional components, was able to bind *nanos1* RNA directly.

To determine if Dnd1 binds *nanos1* mRNA in vivo, we performed ribonucleoprotein immunoprecipitation (RIP) assays on stage 7 embryos. RNAs associated with Dnd1 protein were extracted for RT-PCR. Consistent with the filter binding assay, *nanos1* RNA and Dnd1 co-precipitated from embryo extracts. In addition, Dnd1 associated with a subset of germline specific mRNAs that included *trim36, deadsouth, germes, grip2,* and *syntabulin* (Fig. 3B). Germline specific RNAs not recognized by Dnd1 included *xdazl, xpat, vasa,* and *dnd1* itself. Three somatic determinants were also tested (*vg1*, *vegT*, *wnt11*). Only *vegT* associated with Dnd1 in the assay.

In zebrafish PGCs, Dnd1 antagonizes miRNA through an action that requires a poly-U rich region within the *nanos* 3'UTR (Kedde et al., 2007). Although not directly shown, presumably Dnd1 binds to this region, which is in close proximity to the miRNA recognition site, thereby blocking miRNA accessibility and allowing *nanos* expression. In contrast, previous work in *Xenopus* shows that the 3'UTR is dispensable for repressing *nanos1* translation (Luo et al., 2011). Based on these observations, we asked if the *nanos1* 3'UTR was dispensable for Dnd1 binding and Dnd1-induced *nanos1* translation. To address any requirement of the 3'UTR for Dnd1 binding, the full-length *nanos1* RNA (*nanos1-nanos1 $^{3'}$UTR*), *nanos1* lacking its own 3'UTR (*nanos1-ß-globin $^{3'}$UTR*, (Luo et al., 2011)), and *GFP* RNA, used as a negative control, were incubated with GST-Dnd1 protein. Bound RNAs were pulled down with GST-Dnd1 then analyzed by qPCR. We found that GST-Dnd1 effectively bound both the *nanos1-ß-globin $^{3'}$UTR* and *nanos1-nanos1 $^{3'}$UTR*, but not *GFP* (Fig. 3C). In parallel with the RNA binding assay, we also investigated the requirement of the *nanos1* 3'UTR on Dnd1-induced *nanos1* translation in stage VI oocytes. Translation of *nanos1-ß-globin $^{3'}$UTR*, like *nanos1-nanos1 $^{3'}$UTR*, was barely detected in oocytes. However, in the presence of Dnd1 protein, both transcripts were now translated (Fig. 3D). Thus, the 3'UTR of *nanos1* is not required for Dnd1 to promote *nanos1* translation. Taken together, we concluded that Dnd1 promotes *nanos1* translation through binding the ORF of *nanos1* mRNA.

Dnd1 physically interacts with eIF3f

Based on our finding that Dnd1 could activate *nanos1* translation in wheat germ extracts, we hypothesized that Dnd1 may interact with a general translation factor to regulate *nanos1* translation. To identify Dnd1 interacting partners and gain mechanistic insight, we screened a yeast-2-hybrid library containing cDNAs from 7-day mouse embryos using *X. tropicalis* Dnd1 as bait. We identified the eukaryotic initiation factor 3 subunit f (eIF3f) as a Dnd1 interacting protein (data not shown). The interaction was confirmed by co-IP with FLAG-eIF3f and myc-Dnd1 in HEK293T cells (Fig 4A, lanes 6, 11, 12). To extend and confirm these findings, we generated various Dnd1 deletion constructs and identified two eIF3f-binding domains in Dnd1 protein. These domains are located between residues 96-127 and 305-C-terminus (Supplemental Fig. 2). The binding between Dnd1 and eIF3f was not affected by RNase A treatment, suggesting that the formation of the Dnd1-eIF3f complex did not require RNA to be present (Fig. 4A, compare lanes 11, 12). In addition, myc-Dnd1 bound endogenous eIF3f in HEK293T cells (Fig. 4B). Taken together, these results showed that endogenous eIF3f can interact with Dnd1 protein.

eIF3f is one of 13 subunits within the eIF3 complex, a protein complex associated with the 40S ribosomal subunit in the 43S Pre-Initiation Complex (PIC) that binds to the 5' proximal region of mRNAs. The finding that Dnd1 interacts with eIF3f immediately raised the possibility that Dnd1 interacts with the eIF3 complex through this subunit to promote *nanos1* translation. To begin testing this hypothesis, we asked if Dnd1 could pull down other core components of eIF3, namely eIF3m and eIF3h (reviewed in (Marchione et al., 2013)). We transfected HEK293T cells with either FLAG-eIF3m or FLAG-eIF3h with myc-Dnd1 then performed co-IP by

immunoprecipitation with myc. Myc-Dnd1 did bring down FLAG-eIF3m and eIF3h, suggesting that Dnd1 interacts with the eIF3 complex (Fig. 4C, lanes 2, 4).

To further test an association between *Xenopus* endogenous Dnd1 and the eIF3 complex, we carried out sucrose gradient analyses at two different developmental time points: 1) in ovulated eggs, when Dnd1 is expressed at extremely low levels, and 2) in early cleavage stage embryos (32-cell), when Dnd1 expression is high (Figs. 2B). The presence of Dnd1, eIF3f, and eIF3c was determined for each gradient fraction by Western blot. The large scaffold subunit eIF3c is integral to the eIF3 complex and therefore served as the marker for the complex. As expected, eIF3c was only found in the two highest density fractions (Fig. 5A). The expression of Dnd1 was very low in ovulated eggs and was not detected with eIF3c in fractions 1 and 2, not even after IP with Dnd1 antibody (data not shown). In embryos, however, a fraction of Dnd1 and eIF3f co-migrated in the two highest density fractions with eIF3c. In addition to Dnd1 co-migrating with large protein complexes in the highest density fractions, we detected a portion of the Dnd1 within the medium to low density fractions of the gradient (Fig. 5A; fractions 8-11). To determine if Dnd1 and eIF3f were directly interacting in the eIF3 complex, the heaviest sucrose fractions 1 and 2 from embryo extracts were combined and endogenous Dnd1 was immunoprecipitated. In parallel, we combined fractions 8, 9, and 10 and immunoprecipitated endogenous Dnd1. Precipitates were tested for the presence of eIF3f by Western blot. We found that eIF3f was co-immunoprecipitated with Dnd1 in fractions 1 and 2, but not in fraction 8, 9, and 10 (Fig. 5B). Collectively, the above results suggest that endogenous Dnd1, through binding eIF3f, interacts with the eIF3 complex in early embryos, exactly at the time when *nanos1* is translated.

Dnd1 functionally interacts with eIF3f

If eIF3f and Dnd1 interact functionally within the germline, we should be able to detect an effect on PGCs if such an interaction is disrupted. The maternal supply of eIF3f protein and RNA present in the egg and embryo makes a traditional knockdown approach impractical. Furthermore, depletion of eIF3f would likely affect the stability and function of the eIF3 complex and subsequently the 43S PIC, causing non-specific effects (Hinnebusch, 2006; Lomakin and Steitz, 2013; Pestova et al., 2001; Sun et al., 2011). To circumvent these problems, we set out to map the minimal Dnd1 binding domain of eIF3f. We hypothesized that overexpression of the minimal Dnd1 binding domain of eIF3f would sequester endogenous Dnd1 and disrupt the Dnd1-eIF3f complex *in vivo*.

As shown in Fig. 6A and B, the minimal Dnd1-binding domain in eIF3f was mapped to residues 92-200. The eIF3f$^{92\text{-}200}$ fragment was tested for its ability to compete with endogenous eIF3f for Dnd1 binding. Myc-Dnd1 and FLAG-eIF3f were transfected into HEK293T cells together with an increasing amount of eIF3f$^{92\text{-}200}$. CoIP with myc antibody revealed a decline in eIF3f binding to Dnd1 as levels of eIF3f$^{92\text{-}200}$ increased (Fig. 6C). Thus, overexpression of eIF3f$^{92\text{-}200}$ disrupted the Dnd1-eIF3f complex in a dose dependent fashion. It is important to note that overexpression of eIF3f, Dnd1, and eIF3f$^{92\text{-}200}$ did not affect the growth and viability of HEK293T cells (data not shown). Importantly, overexpression of eIF3f$^{92\text{-}200}$ disrupted the interaction between Dnd1 and eIF3h as well (Fig. 6D), providing strong support for our conclusion that Dnd1, through binding eIF3f, interacts with eIF3. These results demonstrate that eIF3f$^{92\text{-}200}$ can be used as a dominant negative form of eIF3f to disrupt the interaction between eIF3f and Dnd1 specifically.

We next asked if interfering with the eIF3f-Dnd1 complex would affect *nanos1* translation and PGC development. The expression of endogenous Nanos1 is below the level of detection by Western blot. Therefore, to assess the effect of eIF3f$^{92\text{-}200}$ on *nanos1* translation, we injected *nanos1* RNA alone or together with *eIF3f*$^{92\text{-}200}$ into fertilized eggs. Uninjected fertilized eggs served as controls. We immunoprecipitated Nanos1 in stage 11 embryos, allowing sufficient time for translation to have occurred. As shown in Fig. 6E, indeed, overexpression of eIF3f$^{92\text{-}200}$ reduced the expression of Nanos1 protein. This inhibition was relieved by coexpression of eIF3f$^{92\text{-}200}$ with myc-Dnd1, which can titrate out overexpressed eIF3f$^{92\text{-}200}$. To assess the effect of eIF3f$^{92\text{-}200}$ on PGC development, we injected *eIF3f*$^{92\text{-}200}$ into the vegetal pole of fertilized eggs and collected embryos at late tailbud (stage 33), and performed *in situ* hybridization with *Xpat* probe to detect PGCs (Hudson and Woodland, 1998). As shown in Fig. 7A-D, embryos injected with *eIF3f*$^{92\text{-}200}$ appeared normal morphologically, but showed reduced numbers of PGCs. Importantly, this effect of *eIF3f*$^{92\text{-}200}$ was rescued by overexpression of Dnd1. Taken together, these results indicate that the biochemical interaction between Dnd1 and eIF3f is important for *nanos1* translation and PGC development *in vivo*.

eIF3f functions as a repressor of translation

The function of eIF3f within the multi-subunit eIF3 complex is commonly described in the literature as a translational repressor (Marchione et al., 2013). Indeed, we found that overexpression of eIF3f inhibited *nanos1* translation in wheat germ extracts (Fig. 8A). This inhibition was alleviated by addition of purified GST-Dnd1 protein in a dose-dependent manner (Fig. 8A). Overexpression of eIF3f in *Xenopus* embryos also consistently reduced the expression

level of Nanos1 protein (Fig. 8B), without affecting the levels of endogenous or overexpressed *nanos1* mRNAs (Supplemental Fig. 3). Because overexpression of eIF3f reduced Nanos1 expression, and Nanos1 is essential for PGC survival (Lai et al., 2012), we hypothesized that eIF3f overexpression would also effect PGC development. In agreement with this hypothesis, eIF3f overexpressed embryos showed reduced numbers of *Xpat*-positive PGCs compared to uninjected controls (Fig. 8C, D, F). Co-expression of Dnd1 with eIF3f rescued the number of *Xpat*-positive PGCs, confirming the specificity of the effect (Fig. 8E and F). These data further support that Dnd1 functions to relieve the repressive activity of the eIF3 subunit, 3f, on *nanos1* translation within the germline.

Discussion

A fairly detailed understanding of translational control mechanisms that operate in the oocyte has been documented. The role of the cap binding complex eIF4E and its association with eIF4G to promote polyadenylation and translation has been intensely investigated (Richter, 2011). In contrast, very little is known about how maternal RNAs, sequestered in the germ plasm, are translationally activated after fertilization. During *Xenopus* oogenesis, *nanos1* and other maternal RNAs are sequestered within the germ plasm and are translationally activated only after fertilization (Lai et al., 2011; Luo et al., 2011). There is no evidence that the polyA tail of *nanos1* changes significantly during early stages of germline development, suggesting that control of *nanos1* translation is unlikely to be at the level of eIF4. We previously reported that *nanos1* is repressed prior to fertilization through a TCE, which structurally blocks scanning of mRNA by the 43S PIC (Luo et al., 2011). The mechanism that relieves *nanos1* translational repression has not been characterized.

Here we show that Dnd1, a vertebrate-specific germline RNA-binding protein essential for germ cell development (Horvay et al., 2006; Weidinger et al., 2003), is both required and sufficient to activate *nanos1* translation in the early embryo. The expression of Dnd1 protein is entirely consistent with its role in *nanos1* activation: it increases markedly within the germ plasm after fertilization just prior to the detection of Nanos1 protein (Fig. 2; (Mei et al., 2013)). Misexpression of Dnd1 triggers premature *nanos1* translation in the oocyte, resulting in abnormal development (Fig. 1A; (Luo et al., 2011)). Conversely, oocytes depleted of Dnd1 gave rise to embryos that lack Nanos1 protein even though normal levels of *nanos1* RNA were present (Fig.1D, E). No other germline components could compensate for Dnd1 in activating *nanos1* translation.

How does Dnd1 promote *nanos1* translation? Our previous studies reveal that Dnd1 anchors *trim36* RNA to the vegetal cortex in *Xenopus* oocytes and regulates polymerization of cortical microtubule arrays after egg activation (Mei et al., 2013). Much later in development, during gastrulation, zebrafish Dnd1 has been proposed to block microRNA binding to the 3'UTR of *nanos* and other germline RNAs and thus protect them from miRNA-mediated degradation (Kedde et al., 2007; Slanchev et al., 2009). Our results presented here show that Dnd1 promotes *nanos1* translation during early cleavage, at least 6-7 hours before gastrulation when miRNA-mediated degradation of germline specific RNAs occurs. Furthermore, the 3'UTR of *nanos1* is not required for Dnd1 to activate *nanos1* translation. These observations point directly at yet another novel germline function of Dnd1, i.e. promoting translation distinct from miRNA mediated degradation. Indeed, we found that Dnd1 activates *nanos1* translation by directly

binding both *nanos1* RNA and the repressive subunit of the eIF3 complex, eIF3f. Interfering with this novel function of Dnd1 impairs *nanos1* translation and PGC development, without affecting formation of cortical microtubule arrays after egg activation or the stability of germline specific RNAs in embryos (Supplemental Fig. 4). Thus, our data have defined a previously uncharacterized function for Dnd1 and have revealed a novel translational control mechanism operating in the germline unique to vertebrates.

Based on our results and the literature, we propose that Dnd1 plays two important roles during *nanos1* translation. Dnd1 contains ATPase activity (Liu and Collodi, 2010). It is likely that once binding *nanos1* mRNA, Dnd1 functions as a helicase to melt the TCE, or acts as a chaperone recruiting a helicase, which ultimately melts the *nanos1* TCE. Meanwhile, Dnd1 relieves the inhibitory effect of eIF3f in the 43S PIC through its direct interaction with eIF3f, thus promoting initiation. In support of this view, we found that Dnd1 interacted directly with eIF3f and coimmunoprecipitated with overexpressed eIF3m or 3h, two other subunits of the eIF3 complex (Fig. 4C). We were able to show that endogenous Dnd1 co-migrated with eIF3f and the eIF3c core subunit on sucrose gradients (Fig. 5A), demonstrating that Dnd1 associates with eIF3f as part of the eIF3 preinitiation complex (Fig. 5B). It appears that Dnd1 promotes *nanos1* translation through a novel regulatory mechanism occurring at the level of eIF3.

eIF3f is a repressive component of the eIF3 complex (Marchione et al., 2013). Its activity can be regulated through phosphorylation, in which the phosphorylated form represses translation (Shi et al., 2009). Interestingly, Thr119, one of the two phosphorylation sites of eIF3f, lies within the Dnd1 binding domain of eIF3f (residues 92-200) (Fig. 6). It has been reported that Mss4 binds

directly to eIF3f and suppresses the repressive activity of eIF3f by blocking eIF3f phosphorylation (Walter et al., 2012). Future experiments will determine if Dnd1 activates *nanos1* translation through a similar mechanism, i.e., acting as the "neutralizing agent" of eIF3f. Indeed, we found that overexpression of eIF3f suppresses *nanos1* translation and PGC development. Dnd1 relieves the inhibitory effects of eIF3f both *in vivo* and *in vitro*. Our findings are consistent with a model that has Dnd1 binding to both eIF3f and *nanos1* RNA, altering the TCE and promoting subsequent scanning of the 43S PIC (Fig. 8G).

nanos1 RNA is repressed through a steric hindrance mechanism designed for fail-safe long-term sequestration. In addition to *nanos1,* we found that Dnd1 also binds other germline RNAs, including *trim36* (Mei et al., 2013), *deadsouth* (MacArthur et al., 2000), *germes* (Berekelya et al., 2003), *grip2* (Tarbashevich et al., 2007), and *syntabulin* (Colozza and De Robertis, 2014). Intriguingly, we found that overexpression of eIF3f inhibited *deadsouth* translation in wheat germ extracts and addition of GST-Dnd1 protein alleviated this inhibitory effect of eIF3f (Aguero unpublished data). It seems likely that after fertilization, eIF3f-mediated translational repression is relieved by an abrupt increase in the expression of Dnd1 protein. This allows efficient translation of *nanos1* and some other germ line RNAs, initiating the PGC development program. We suggest that Dnd1, by bridging the earliest acting initiation factors and the RNAs, serves to efficiently alter secondary structures of the mRNA and promote translation. Given that Nanos plays critical roles in protecting germ cell fate during early stages of PGC development, we speculate that Dnd1, through regulating translation of nanos1 and other germline RNAs, prevents PGCs from reprogramming into other cell types and maintains the PGC identity. In the

future, it will be important to determine if Dnd1 functions as a general activator of translation to control a subset of germline RNAs.

Taken together, our evidence strongly supports an essential role for Dnd1 in facilitating the translation activation of germline *nanos1* RNA in the embryo. The transition between germline RNA quiescence in the oocyte and activation after fertilization is regulated in part by the balance between Dnd1 and eIF3f activities. Our data support a novel level of translational control within PGCs, that is at the level of the eIF3 complex.

Materials and Methods

Oocyte and embryo micro-injection and host transfer

Oocytes and embryos were obtained as described (Sive et al., 2000). For injection, RNAs were synthesized from linearized plasmids using the mMESSAGE mMACHINE Kit (Ambion). The protocol for *Xenopus* studies (#14249) has been approved by University of Illinois Institutional Animal Care and Use Committee.

Maternal depletion of *dnd1* was performed as described (Mei et al., 2013). Briefly, manually defoliculated oocytes were injected with 7.5 ng of a phosphorothioate-modified antisense oligonucleotide (AS-oligo) (5'-C*C*C*TCGATTCAGGCCA*C*T-3', Integrated DNA Technologies) alone or together with 100 pg of *tropicalis dnd1*, which lacks the AS-oligo binding sequence. Control and injected oocytes were cultured for 24 hours before being matured by treatment with 2.0 μM progesterone. Matured oocytes were colored with vital dyes, transferred to egg-laying host females, recovered and fertilized essentially as described (Mir and Heasman, 2008).

Immunofluorescence and confocal imaging

Immunofluorescence and confocal imaging were performed as described (Mei et al., 2013; Venkatarama et al., 2010). Briefly, embryos were fixed in Dent's (80% methanol and 20% DMSO) for 2 hours and stored in methanol overnight at 4°C. Rehydrated embryos were incubated in blocking buffer (0.2% BSA, 0.1 % Triton X-100 in 1xPBS) with 10% donkey serum for an hour at room temperature, and then stained with anti-Dnd1 (1:100) (Mei et al., 2013), anti-Nanos1 (1:50) (Luo et al., 2011), and anti-Xiwi (1:100) (Lau et al., 2009; Wilczynska et al., 2009) antibodies overnight. Embryos were washed with blocking buffer three times and stained

with anti-goat Alexa-555 and anti-rabbit Alexa-488 fluorescent antibody (Invitrogen) for an hour. Samples were washed again with blocking buffer three times before mounting for fluorescence confocal microscopy.

Purification of GST-Dnd1 protein and in vitro RNA pull down assay

Bacteria (BL21) were transformed with pGEX6p-Dnd1 (Mei et al., 2013) and cultured in LB with IPTG (100 μM) at 30°C for 3 hours before harvesting. Recombinant GST-Dnd1 protein was purified from the lysate using glutathione-agarose beads. Removal of GST was performed on the column with PreScission Protease (80 units/ml) according to manufacturer's instructions (GE Health).

For the *in vitro* RNA pull down assay, GST-Dnd1-bound glutathione beads were incubated with 10 μg yeast tRNA in 1ml RIP buffer (50 mM Tris pH7.6, 125 mM NaCI, 1 mM EDTA, 0.25% NP-40, 0.2% glycerol, 0.1 mM DTT, and 100 U/ml RNasin) at 4°C for 1 hour for pre-absorption. 100 ng synthesized mRNAs were added to 1ml RIP buffer containing pre-absorbed beads and incubated for an additional 4 hours at 4°C. The mixture was then centrifuged and 50 μl supernatants were set aside as "5% of mRNA input". Beads were washed five times with RIP buffer and once with RIP buffer without NP-40 and DTT (50 mM Tris pH7.6, 125 mM NaCl, 1 mM EDTA, 0.2% glycerol, and 100 U/ml RNasin). mRNAs were recovered from beads using Trizol reagent for cDNA synthesis and subsequent qPCR. The ratio between pulled down mRNA and 5% of mRNA input was used to determine binding of mRNAs by GST-Dnd1. GST served as the negative control. Primers for *nanos1* are 5'-gggaggcgctgtctctatac-3' and 5'-

ctctggggatctctgaggag-3'. Primers for GFP are 5'-ctgaagttcatctgcaccac-3' and 5'-gtccttgaagaagatggtgc-3'.

Filter binding assay

The double-filter binding assay was performed as described (Vincent and Deutscher, 2006). Briefly, the nitrocellulose membrane was soaked in 0.5 M KOH for 10 min followed by a H_2O rinse. The nylon membrane was then sequentially soaked in 0.1 M EDTA (pH 8.8) for 10 min, 1M KCl three times, 10 min for each, 0.5 M KOH for 1 min followed by H_2O rinse. Both membranes were then equilibrated in the binding buffer (20 mM Tris-HCl pH8.0, 100 mM KCl, 1 mM DTT, 10 mM EDTA, 10% glycerol) for at least 1 hour before use. The binding reaction was set up with 20 pmol ^{32}P-labeled RNA substrate and varying amounts of Dnd1 protein in binding buffer and incubated on ice for 30 min. No Dnd1 protein added served as the negative control. The membranes were assembled onto a 96-well dot-blot apparatus (Bio-Rad) so that the reaction solutions went through the nitrocellulose and nylon sequentially by vacuum force. The membranes were allowed to air dry and visualized by PhosphoImager (Molecular Dynamics). Quantification of the ^{32}P signal was carried out with ImageQuant. Recombinant Dnd1 used in this assay lacks the first 51 amino acids residues (Horvay et al., 2006; Koebernick et al., 2010).

Ribonucleoprotein immunoprecipitation (RIP) assay

Xenopus embryos were collected at stage 7 (50 embryos per tube, 8 tubes in total), washed twice with cold wash buffer (50mM Tris pH7.6, 125mM NaCl, 1mM EDTA), and lysed in 0.5ml of lysis buffer (50mM Tris pH7.6, 1 25mM NaCl, 1 mM EDTA, 0.75% NP-40, 0.3mM DTT,

100U/ml RNasin) by pipetting. 1 ml of cold wash buffer with 1 U/ml RNasin and 0.6% glycerol was added into each tube. This brought the final concentration to 50 mM Tris pH7.6, 125 mM NaCl, 1 mM EDTA, 0.25% NP-40, 0.2% glycerol, 0.1 mM DTT, and 100 U/ml RNasin, which is essentially the same as the RIP buffer. After centrifugation, cleared lysates were combined into 15 ml tubes (total 2 tubes, each containing 6 ml lysate made from 200 embryos) and mixed gently. 60 µL of the lysate was set aside as "1% RNA input". Dnd1 antibody or normal rabbit IgG, and 6 µl of TURBO DNase (AM2238, Ambion) was added into each tube followed by gentle rotation in the cold room for 4 hours. In parallel, 200 µl Dynabeads Protein G (Life Technologies) was washed with 1 ml cold RIP buffer (50 mM Tris pH7.6, 125 mM NaCl, 1 mM EDTA, 0.25% NP-40, 0.2% glycerol, 0.1 mM DTT, and 100 U/ml RNasin) three times. After washing, 1 ml RIP buffer was added to the beads. RIP and negative control samples were centrifuged twice at the maximal speed at 4°C for 10 min. The supernatants were transferred into clean tubes. 450 µl Dynabeads were added into each tube and rotated gently in the cold room for 1 hour. Samples were then transferred into 1.5 ml tubes and washed with RIP buffer four times. Beads were then washed with 1 ml RIP buffer without NP-40 and DTT (50 mM Tris pH7.6, 125 mM NaCl, 1 mM EDTA, 0.2% glycerol, and 100 U/ml RNasin). RNAs associated with beads were extracted using Trizol reagent and resuspended in 20 µl water. cDNAs were synthesized using 5 µl of RNA solution. PCR primers were: *trim36*, 5'-aagtcctctcatgttgcagg-3' and 5'-aacctcctccagatgtatgg-3'. *deadsouth*, 5'-ttctcaaaagctgtcggatgac-3' and 5'-ctactgagccatcaacatttactgg-3'. *germes*, 5'-ttctgtgcattggcagcaagactg-3' and 5'-tcttctgtatgtcctggttctgcag-3'. *grip2*, 5'-gaccttgaaacatgtggacagtcag-3' and 5'-tgttgctgctgatgtgatggcttcc-3'. *syntabulin*, 5'-tacttgaggaccaagcaacggag-3' and 5'-cttgttccatccagtgtgaactttgg-3'. *Xdazl*, 5'-gttcaggcttgcccatatccaag-3' and 5'-

ttggatccatatcacagcagtgg-3'. *vasa*, 5'-catcaacaagcattcacggtg-3' and 5'-ccaattctatggacgtactcatc-3'. *VegT*, 5'-caagtaaatgtgagaaaccg-3' and 5'-caaatacacacacatttccc-3'. *Vg1*, 5'-atgcctattgcttctatttgc-3' and 5'-ggtttacgatggtttcactca-3'. *dnd1*, 5'-tggtaatgctccagtcagtg-3' and 5'-taagcgaaccctcgattcag-3'. *Xpat*, 5'-tctgaagttctgtggagctgc-3' and 5'-ttagcccacagttggaagagg-3'. *nanos1*, 5'-tgagtctgtgggacacaaagg-3' and 5'-actctggggatctctgaggag-3'. *wnt11*, 5'-gaagtcaagcaagtctgctgg-3' and 5'-gcagtagtcaggggaactaaccag-3'.

Quantitative RT-PCR

RNA was extracted from samples using Trizol reagent (Life Technologies). PCR was performed using Power SYBR Green Master Mix (Life Technologies) on an Applied Biosystems 7500 real-time PCR system. Values were normalized to *ornithine decarboxylase* (*odc)*. Statistical significance was determined by Student's t-test. Results are presented as mean ±s.d. PCR primers were as listed for RIP; *odc*, 5'-cagctagctgtggtgtgg-3' and 5'-caacatggaaactcacacc-3'.

In vitro translation

In vitro translation was carried out using wheat germ extracts according to the manufacturer's instructions (Promega). 0.5 µg capped-mRNA and GST-Dnd1 protein were used per reaction.

Yeast two-hybrid screen

A mouse 7-day embryo cDNA library (Clontech) was screened using full-length *Xenopus* Dnd1 (pGBKT7-xDnd1) as bait, according to standard protocols (Yeast Protocols Handbook, Clontech).

Plasmids

ORFs of mouse eIF3f, eIF3h and eIF3m were cloned by RT-PCR from mouse embryonic fibroblasts. *Xenopus* eIF3f ORF was cloned by RT-PCR from *Xenopus laevis* stage VI oocytes. All full-length and deletion constructs were generated by PCR and cloned into pCS2+ and sequenced.

Cell culture, transfection, co-IP and Western blot

HEK293T cells, which were authenticated and tested for contamination, were cultured and transfected as described (Jin et al., 2009)**.** Protocols for CoIP and Western blot were described (Jin et al., 2009). Antibodies are: anti-myc (#5546, Sigma-Aldrich, 1:1,000), anti-FLAG (#F1804, Sigma-Aldrich, 1:1,000), anti-β-tubulin (#T5293, Sigma-Aldrich, 1:2,500), anti-Dnd1 ((Mei et al., 2013), 1:500), anti-Nanos1 ((Luo et al., 2011), 1:500), anti-Vasa (H80, sc-67185, Santa Cruz, 1:500), anti-Xiwi ((Lau et al., 2009), 1:1,000), anti-Pumilio2 (A300-202A, Bethyl Labs, 1:1,000), anti-mouse eIF3f (#390413, Santa Cruz, 1:500), and anti-eIF3c (sc-74507, Santa Cruz, 1:500).

Sucrose Gradient analysis

The sedimentation properties of Dnd1, eIF3f and eIF3c from total ovulated egg (OE) and 32-cell stage embryo extracts were analyzed in sucrose gradients essentially as follows: 350 OE or 32-cell stage embryos were collected from four different frogs and lysed in lysis buffer containing 50mM Tris-HCl pH 7.5, 150 mM NaCl, 1% NP40, and 4X ROCHE protease inhibitor cocktail. After centrifugation (2X 14,000 rpm/15min/4°C), approximately 500ul of extract was collected from each sample. Internal standards lactate dehydrogenase (LDH, 130 kDa) (Sigma) and

hemoglobin (67 kDa) were dissolved in 40ul lysis buffer and mixed with 450 ul of each sample. Samples (~500ul) were applied to 5ml of a linear 7-20% sucrose gradient made in lysis buffer. Centrifugation was for 13.5 hr at 45,500 RPM with slow acceleration and brake off using Beckman SW55 Ti rotors. Gradients were collected in 14 equal fractions of approximately 350ul each. 25 µl from each fraction was used to detect endogenous Dnd1, eIF3f and eIF3c proteins by Western blot. For IP, fractions 1+2 and 8+9+10 were combined (~300ul total) and incubated with anti-Dnd1 antibody for 3 hrs, followed by incubation with protein G-beads overnight at 4°C. All of the gradients were performed in biological quadruplicates. Fractions containing hemoglobin were detected at 410 nm absorbance. LDH was measured at 340 nm in the presence of NADH and pyruvate using a microplate reader (PROMEGA).

Author Contributions

Conceptualization and Methodology, JY and MLK; Analysis, TA, ZJ, SC., and AK; Manuscript-writing, MLK and JY.

Acknowledgements

We acknowledge Dr. Xueting Luo for his contribution during the early stage of the study. We thank Drs. William C. Merrick (Case Western Reserve University), Nelson Lau (Brandeis University), and Michael Blower (Harvard Medical School) for providing reagents. We are grateful to Antonio Barrientos and Flavia Fontanesi for making their expertise and equipment available for the gradient analysis. Our work was supported by grants R01HL126845 to AK, R21HD072340 and R01GM102397 to MLK, and R01GM111816 to JY.

Competing interests

The authors declare no competing or financial interests.

References

Ahringer, J. and Kimble, J. (1991). Control of the sperm-oocyte switch in Caenorhabditis elegans hermaphrodites by the fem-3 3' untranslated region. *Nature* **349**, 346-348.

Asaoka-Taguchi, M., Yamada, M., Nakamura, A., Hanyu, K. and Kobayashi, S. (1999). Maternal Pumilio acts together with Nanos in germline development in Drosophila embryos. *Nature cell biology* **1**, 431-437.

Berekelya, L. A., Ponomarev, M. B., Luchinskaya, N. N. and Belyavsky, A. V. (2003). Xenopus Germes encodes a novel germ plasm-associated transcript. *Gene Expr Patterns* **3**, 521-524.

Colozza, G. and De Robertis, E. M. (2014). Maternal syntabulin is required for dorsal axis formation and is a germ plasm component in Xenopus. *Differentiation; research in biological diversity* **88**, 17-26.

Curtis, D., Treiber, D. K., Tao, F., Zamore, P. D., Williamson, J. R. and Lehmann, R. (1997). A CCHC metal-binding domain in Nanos is essential for translational regulation. *Embo J* **16**, 834-843.

Dalby, B. and Glover, D. M. (1993). Discrete sequence elements control posterior pole accumulation and translational repression of maternal cyclin B RNA in Drosophila. *Embo J* **12**, 1219-1227.

Deshpande, G., Calhoun, G., Yanowitz, J. L. and Schedl, P. D. (1999). Novel functions of nanos in downregulating mitosis and transcription during the development of the Drosophila germline. *Cell* **99**, 271-281.

Extavour, C. G. and Akam, M. (2003). Mechanisms of germ cell specification across the metazoans: epigenesis and preformation. *Development* **130**, 5869-5884.

Hinnebusch, A. G. (2006). eIF3: a versatile scaffold for translation initiation complexes. *Trends Biochem Sci* **31**, 553-562.

Horvay, K., Claussen, M., Katzer, M., Landgrebe, J. and Pieler, T. (2006). Xenopus Dead end mRNA is a localized maternal determinant that serves a conserved function in germ cell development. *Dev Biol* **291**, 1-11.

Hudson, C. and Woodland, H. R. (1998). Xpat, a gene expressed specifically in germ plasm and primordial germ cells of Xenopus laevis. *Mechanisms of development* **73**, 159-168.

Jaruzelska, J., Kotecki, M., Kusz, K., Spik, A., Firpo, M. and Reijo Pera, R. A. (2003). Conservation of a Pumilio-Nanos complex from Drosophila germ plasm to human germ cells. *Development genes and evolution* **213**, 120-126.

Jin, Z., Shi, J., Saraf, A., Mei, W., Zhu, G. Z., Strack, S. and Yang, J. (2009). The 48-kDa alternative translation isoform of PP2A:B56epsilon is required for Wnt signaling during midbrain-hindbrain boundary formation. *J Biol Chem* **284**, 7190-7200.

Kadyrova, L. Y., Habara, Y., Lee, T. H. and Wharton, R. P. (2007). Translational control of maternal Cyclin B mRNA by Nanos in the Drosophila germline. *Development* **134**, 1519-1527.

Kedde, M., Strasser, M. J., Boldajipour, B., Oude Vrielink, J. A., Slanchev, K., le Sage, C., Nagel, R., Voorhoeve, P. M., van Duijse, J., Orom, U. A., et al. (2007). RNA-binding protein Dnd1 inhibits microRNA access to target mRNA. *Cell* **131**, 1273-1286.

Kloc, M. and Chan, A. P. (2007). Centroid, a novel putative DEAD-box RNA helicase maternal mRNA, is localized in the mitochondrial cloud in Xenopus laevis oocytes. *The International journal of developmental biology* **51**, 701-706.

Koebernick, K., Loeber, J., Arthur, P. K., Tarbashevich, K. and Pieler, T. (2010). Elr-type proteins protect Xenopus Dead end mRNA from miR-18-mediated clearance in the soma. *Proc Natl Acad Sci U S A* **107**, 16148-16153.

Lai, F., Singh, A. and King, M. L. (2012). Xenopus Nanos1 is required to prevent endoderm gene expression and apoptosis in primordial germ cells. *Development* **139**, 1476-1486.

Lai, F., Zhou, Y., Luo, X., Fox, J. and King, M. L. (2011). Nanos1 functions as a translational repressor in the Xenopus germline. *Mechanisms of development* **128**, 153-163.

Lau, N. C., Ohsumi, T., Borowsky, M., Kingston, R. E. and Blower, M. D. (2009). Systematic and single cell analysis of Xenopus Piwi-interacting RNAs and Xiwi. *Embo J* **28**, 2945-2958.

Liang, L., Diehl-Jones, W. and Lasko, P. (1994). Localization of vasa protein to the Drosophila pole plasm is independent of its RNA-binding and helicase activities. *Development* **120**, 1201-1211.

Liu, W. and Collodi, P. (2010). Zebrafish dead end possesses ATPase activity that is required for primordial germ cell development. *FASEB journal : official publication of the Federation of American Societies for Experimental Biology* **24**, 2641-2650.

Lomakin, I. B. and Steitz, T. A. (2013). The initiation of mammalian protein synthesis and mRNA scanning mechanism. *Nature* **500**, 307-311.

Luo, X., Nerlick, S., An, W. and King, M. L. (2011). Xenopus germline nanos1 is translationally repressed by a novel structure-based mechanism. *Development* **138**, 589-598.

MacArthur, H., Houston, D. W., Bubunenko, M., Mosquera, L. and King, M. L. (2000). DEADSouth is a germ plasm specific DEAD-box RNA helicase in Xenopus related to eIF4A. *Mechanisms of development* **95**, 291-295.

Marchione, R., Leibovitch, S. A. and Lenormand, J. L. (2013). The translational factor eIF3f: the ambivalent eIF3 subunit. *Cellular and Molecular Life Sciences* **70**, 3603-3616.

Mei, W., Jin, Z., Lai, F., Schwend, T., Houston, D. W., King, M. L. and Yang, J. (2013). Maternal Dead-End1 is required for vegetal cortical microtubule assembly during Xenopus axis specification. *Development* **140**, 2334-2344.

Mir, A. and Heasman, J. (2008). How the mother can help: studying maternal Wnt signaling by anti-sense-mediated depletion of maternal mRNAs and the host transfer technique. *Methods Mol Biol* **469**, 417-429.

Mosquera, L., Forristall, C., Zhou, Y. and King, M. L. (1993). A mRNA localized to the vegetal cortex of Xenopus oocytes encodes a protein with a nanos-like zinc finger domain. *Development* **117**, 377-386.

Murata, Y. and Wharton, R. P. (1995). Binding of pumilio to maternal hunchback mRNA is required for posterior patterning in Drosophila embryos. *Cell* **80**, 747-756.

Nakahata, S., Katsu, Y., Mita, K., Inoue, K., Nagahama, Y. and Yamashita, M. (2001). Biochemical identification of Xenopus Pumilio as a sequence-specific cyclin B1 mRNA-binding protein that physically interacts with a Nanos homolog, Xcat-2, and a cytoplasmic polyadenylation element-binding protein. *J Biol Chem* **276**, 20945-20953.

Pestova, T. V., Kolupaeva, V. G., Lomakin, I. B., Pilipenko, E. V., Shatsky, I. N., Agol, V. I. and Hellen, C. U. (2001). Molecular mechanisms of translation initiation in eukaryotes. *Proc Natl Acad Sci U S A* **98**, 7029-7036.

Richter, D. a. L., P (2011). Translational control in oocyte development. *Cold Spring Harbor Perspectives in Biology* **3**, a002758.

Rogers, G. W., Jr., Komar, A. A. and Merrick, W. C. (2002). eIF4A: the godfather of the DEAD box helicases. *Progress in nucleic acid research and molecular biology* **72**, 307-331.

Saitou, M. (2009). Germ cell specification in mice. *Current opinion in genetics & development* **19**, 386-395.

Sato, K., Hayashi, Y., Ninomiya, Y., Shigenobu, S., Arita, K., Mukai, M. and Kobayashi, S. (2007). Maternal Nanos represses hid/skl-dependent apoptosis to maintain the germ line in Drosophila embryos. *Proc Natl Acad Sci U S A* **104**, 7455-7460.

Schaner, C. E., Deshpande, G., Schedl, P. D. and Kelly, W. G. (2003). A conserved chromatin architecture marks and maintains the restricted germ cell lineage in worms and flies. *Dev Cell* **5**, 747-757.

Shi, J., Hershey, J. W. and Nelson, M. A. (2009). Phosphorylation of the eukaryotic initiation factor 3f by cyclin-dependent kinase 11 during apoptosis. *FEBS Lett* **583**, 971-977.

Sive, H., Grainger, R. and Harland, R. (2000). *Early Development of Xenopus laevis; A Laboratory Manual* (1st edn). Cold Spring Harbor: Cold Spring Harbor Press.

Slanchev, K., Stebler, J., Goudarzi, M., Cojocaru, V., Weidinger, G. and Raz, E. (2009). Control of Dead end localization and activity--implications for the function of the protein in antagonizing miRNA function. *Mechanisms of development* **126**, 270-277.

Sonoda, J. and Wharton, R. P. (1999). Recruitment of Nanos to hunchback mRNA by Pumilio. *Genes Dev* **13**, 2704-2712.

---- (2001). Drosophila Brain Tumor is a translational repressor. *Genes Dev* **15**, 762-773.

Strome, S. and Lehmann, R. (2007). Germ versus soma decisions: lessons from flies and worms. *Science* **316**, 392-393.

Strome, S. and Updike, D. (2015). Specifying and protecting germ cell fate. *Nature reviews. Molecular cell biology* **16**, 406-416.

Sun, C., Todorovic, A., Querol-Audi, J., Bai, Y., Villa, N., Snyder, M., Ashchyan, J., Lewis, C. S., Hartland, A., Gradia, S., et al. (2011). Functional reconstitution of human eukaryotic translation initiation factor 3 (eIF3). *Proc Natl Acad Sci U S A* **108**, 20473-20478.

Suzuki, A., Niimi, Y., Shinmyozu, K., Zhou, Z., Kiso, M. and Saga, Y. (2016). Dead end1 is an essential partner of NANOS2 for selective binding of target RNAs in male germ cell development. *EMBO Rep* **17**, 37-46.

Takeda, Y., Mishima, Y., Fujiwara, T., Sakamoto, H. and Inoue, K. (2009). DAZL relieves miRNA-mediated repression of germline mRNAs by controlling poly(A) tail length in zebrafish. *PLoS ONE* **4**, e7513.

Tarbashevich, K., Koebernick, K. and Pieler, T. (2007). XGRIP2.1 is encoded by a vegetally localizing, maternal mRNA and functions in germ cell development and anteroposterior PGC positioning in Xenopus laevis. *Dev Biol* **311**, 554-565.

Venkatarama, T., Lai, F., Luo, X., Zhou, Y., Newman, K. and King, M. L. (2010). Repression of zygotic gene expression in the Xenopus germline. *Development* **137**, 651-660.

Vincent, H. A. and Deutscher, M. P. (2006). Substrate recognition and catalysis by the exoribonuclease RNase R. *J Biol Chem* **281**, 29769-29775.

Walter, B. M., Nordhoff, C., Varga, G., Goncharenko, G., Schneider, S. W., Ludwig, S. and Wixler, V. (2012). Mss4 protein is a regulator of stress response and apoptosis. *Cell death & disease* **3**, e297.

Weidinger, G., Stebler, J., Slanchev, K., Dumstrei, K., Wise, C., Lovell-Badge, R., Thisse, C., Thisse, B. and Raz, E. (2003). dead end, a novel vertebrate germ plasm component, is required for zebrafish primordial germ cell migration and survival. *Curr Biol* **13**, 1429-1434.

Wharton, R. P. and Struhl, G. (1991). RNA regulatory elements mediate control of Drosophila body pattern by the posterior morphogen nanos. *Cell* **67**, 955-967.

Wilczynska, A., Minshall, N., Armisen, J., Miska, E. A. and Standart, N. (2009). Two Piwi proteins, Xiwi and Xili, are expressed in the Xenopus female germline. *Rna-a Publication of the Rna Society* **15**, 337-345.

Wreden, C., Verrotti, A. C., Schisa, J. A., Lieberfarb, M. E. and Strickland, S. (1997). Nanos and pumilio establish embryonic polarity in Drosophila by promoting posterior deadenylation of hunchback mRNA. *Development* **124**, 3015-3023.

Wylie, C. (1999). Germ cells. *Cell* **96**, 165-174.

Yamaji, M., Jishage, M., Meyer, C., Suryawanshi, H., Der, E., Yamaji, M., Garzia, A., Morozov, P., Manickavel, S., McFarland, H. L., et al. (2017). DND1 maintains germline stem cells via recruitment of the CCR4-NOT complex to target mRNAs. *Nature* **543**, 568-572.

Zhang, B., Gallegos, M., Puoti, A., Durkin, E., Fields, S., Kimble, J. and Wickens, M. P. (1997). A conserved RNA-binding protein that regulates sexual fates in the C. elegans hermaphrodite germ line. *Nature* **390**, 477-484.

Zhou, Y. and King, M. L. (1996). Localization of Xcat-2 RNA, a putative germ plasm component, to the mitochondrial cloud in Xenopus stage I oocytes. *Development* **122**, 2947-2953.

Figures

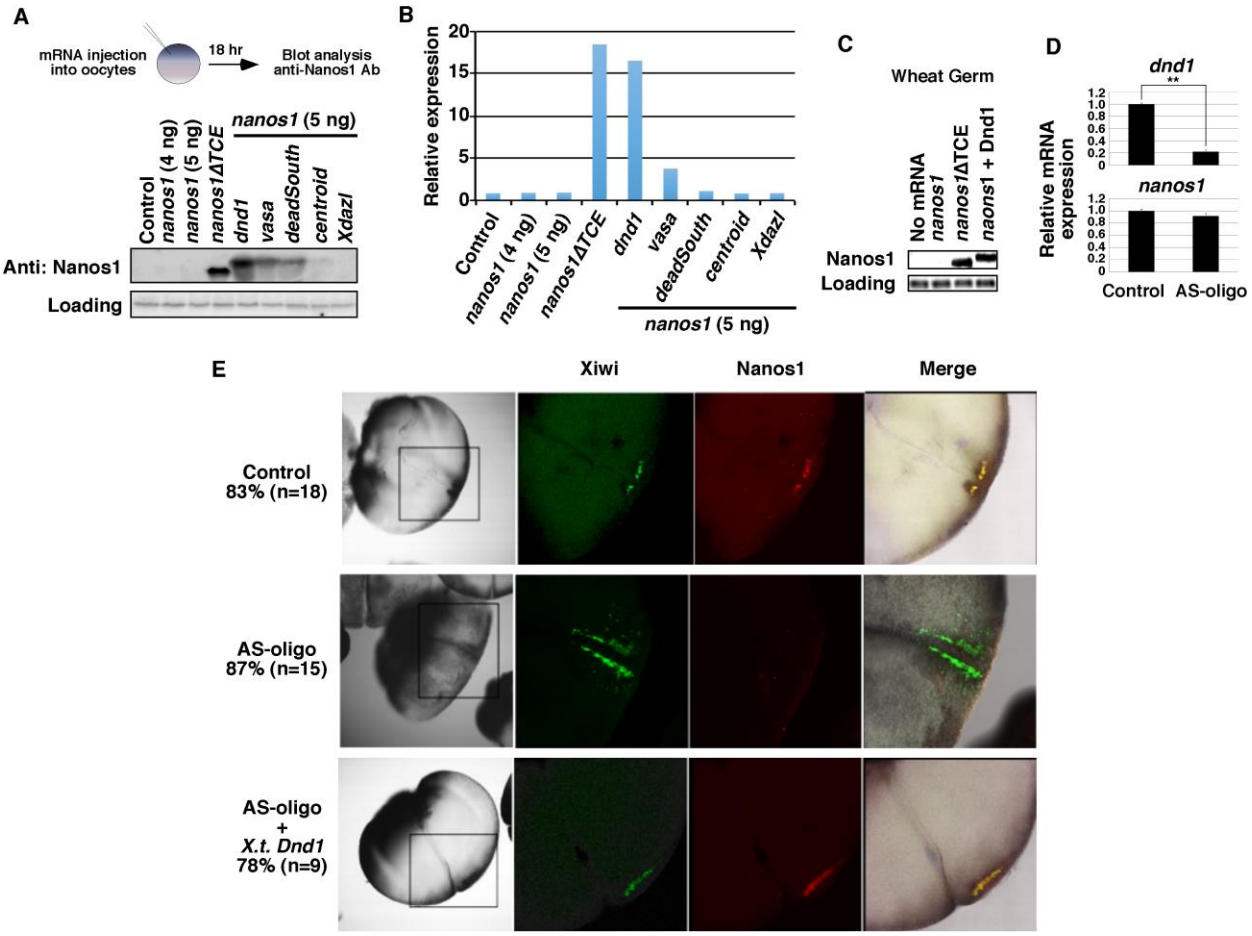

Figure 1. Dnd1 is necessary and sufficient for *nanos1* translation. (A) *nanos1* (4 or 5 ng) was injected into oocytes with or without RNAs encoding Dnd1, Vasa, DeadSouth, Centroid, and Xdazl, each at 2 ng. Nanos1 protein was immunoprecipitated and analyzed by Western blot. *nanos1ΔTCE* served as a positive control for *nanos1* translation. The size difference between Nanos1ΔTCE and the wild type Nanos1 is due to the deletion of the TCE **,** which is located immediately downstream of the translation initiation site. Experiments were repeated for five times. **(B)** Quantification of band intensity of the Western blot in panel **A** using ImageJ. **(C)**

nanos1 RNA was added to wheat germ extracts with or without purified Dnd1 protein. Samples were analyzed for Nanos1 protein expression by Western blot. *nanos1ΔTCE* served as a positive control. Experiments were repeated twice. **(D)** qPCR shows the levels of *dnd1* and *nanos1* in control and *dnd1*-depleted embryos ((AS-oligo) at the 8-cell stage. Data is shown as mean ± s.d. **p<0.01. Experiments were repeated for three times. **(E)** Representative IF images show attenuation of endogenous Nanos1 protein expression by antisense depletion of maternal *dnd1* (AS-oligo). Embryos were co-stained for Xiwi (green) and Nanos1 (red) at the 8-16 cell stage. Experiments were repeated twice.

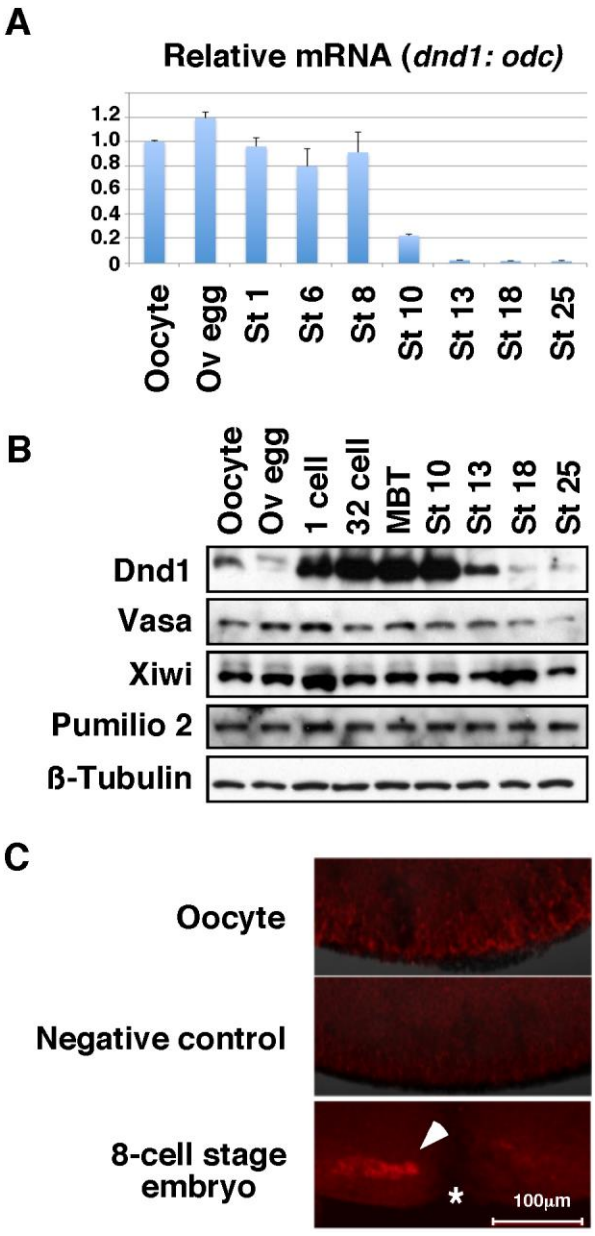

Figure 2. Dnd1 expression pattern. (A) RT-PCR shows the expression of *dnd1* RNA during early development. The experiment was performed twice. **(B)** Western blot showing expression of germline proteins during development, ß-Tubulin was used as a loading control. Dnd1 was IP enriched from 50 oocytes or embryos before Western blotting. All other proteins were detected

using protein extracts from 1/8 oocyte or embryo. The experiment was repeated three times. **(C)** Representative IF images show localization of endogenous Dnd1 protein (red) in oocyte (top, n=7) and 8-cell stage embryo (bottom, n=7). *dnd1* knockdown oocyte (AS-oligo injected) served as a negative control for the specificity of Dnd1 staining (middle, n=10). Oocytes and embryos were hemi-sectioned. Images show the vegetal pole of oocytes or embryo. "*" marks the cleavage furrow of the embryo. Arrow head indicates the germ plasm. St, stage. Ov, ovulated.

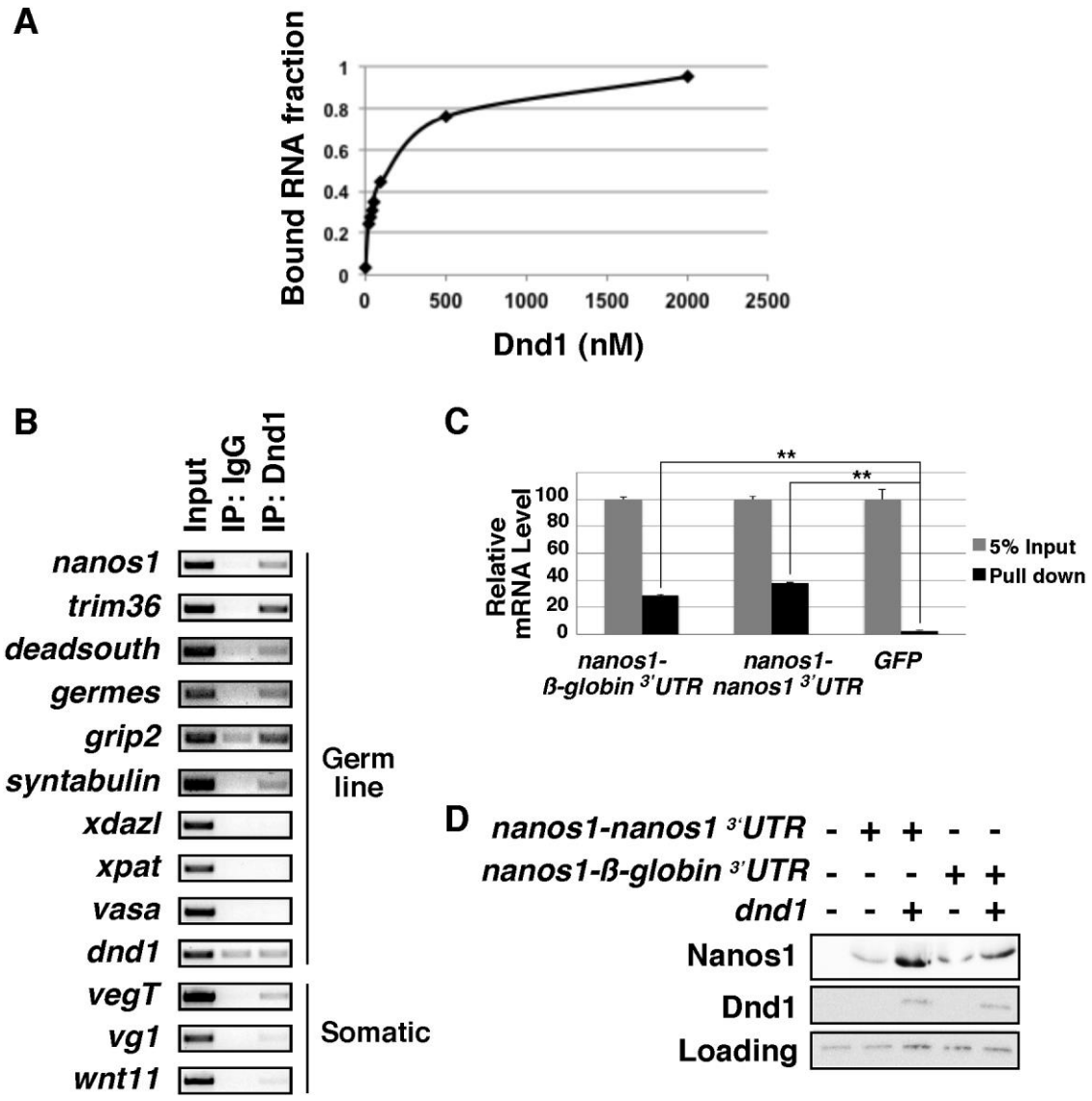

Figure 3. Dnd1 binds *nanos1* RNA. (A) Double-filter nucleic acid binding assay shows recombinant Dnd1 protein binds *nanos1* RNA. The experiment was repeated twice. **(B)** RIP assay followed by RT-PCR shows endogenous Dnd1 protein selectively binds a subset of germline RNAs in stage 7 embryos. The experiment was performed three times. **(C)** RNAs were pulled down by GST-Dnd1 and measured by qPCR. Ratio between the pulldown and 5% of RNA input is shown. *GFP* served as a negative control. Data is shown as mean ± s.d. **p<0.01.

The experiment was repeated four times. **(D)** *nanos1-nanos1 3'UTR* and *nanos1-ß-globin 3'UTR* were injected into stage VI oocytes with or without *dnd1* mRNA. Nanos1 protein was immunoprecipitated and analyzed by Western blot for Nanos1 and Dnd1. The experiment was repeated twice.

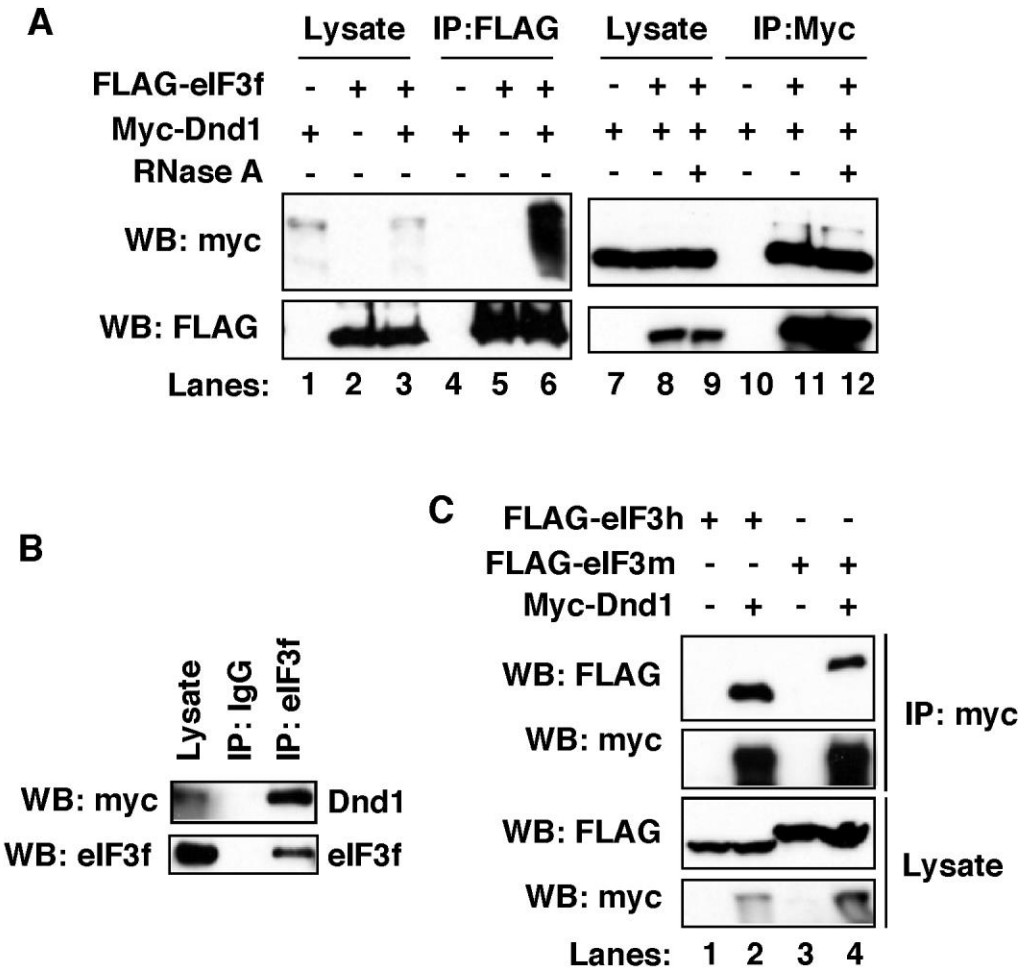

Figure 4. Dnd1 physically interacts with eIF3f. (A) Anti-FLAG (lanes 4-6) or anti-Myc (lanes 10-12) antibodies was used to IP eIF3f or Dnd1 from cell lysates (lanes 9,12). Addition of RNaseA to lysates did not disrupt the Dnd1-eIF3f complex (lane 12). **(B)** Co-IP shows the interaction between myc-Dnd1 and endogenous eIF3f in HEK293T cells. IgG served as negative control. **(C)** Co-IP shows that myc-Dnd1 formed complexes with FLAG-eIF3h and FLAG-eIF3m in HEK293T cells. Experiments were repeated for three times.

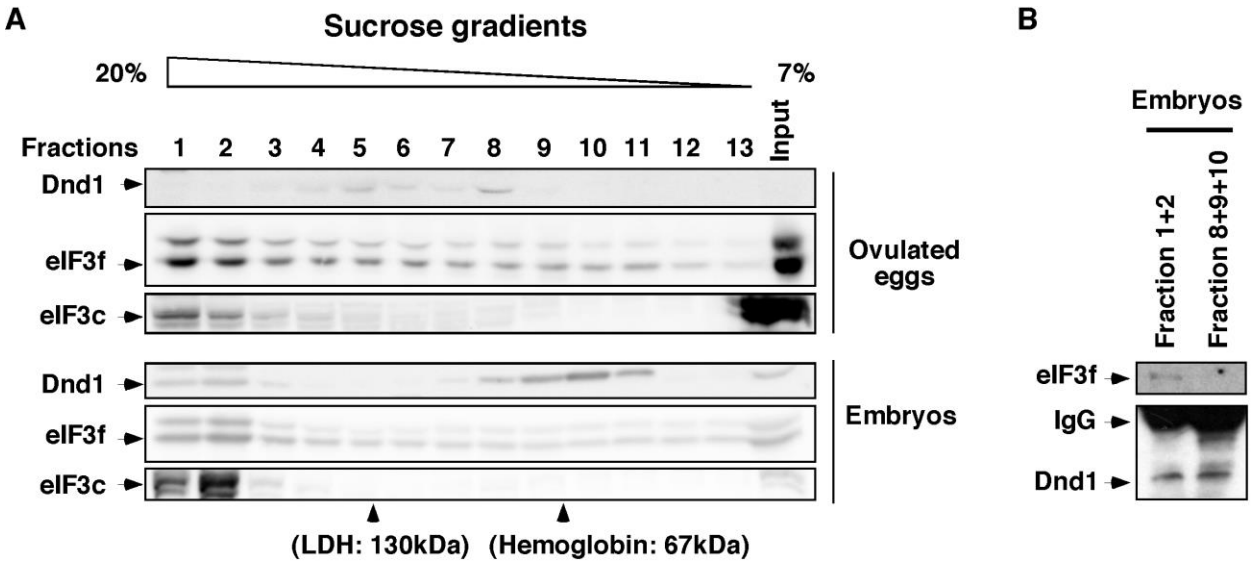

Figure 5. Interaction between endogenous Dnd1 and eIF3f in *Xenopus* embryos. (A) Egg or embryo extracts were fractionated on 7-20% sucrose gradients. Gradient fractions were blotted with antibodies for Dnd1, eIF3f, and eIF3c proteins. Experiments were repeated four times. **(B)** Fractions 1+2 and fraction 8+9+10 of embryo extracts from the sucrose gradients were pooled and immunoprecipitated with an anti-Dnd1 antibody. Endogenous eIF3f and Dnd1 proteins were monitored by Western blot. Experiments were repeated for three times.

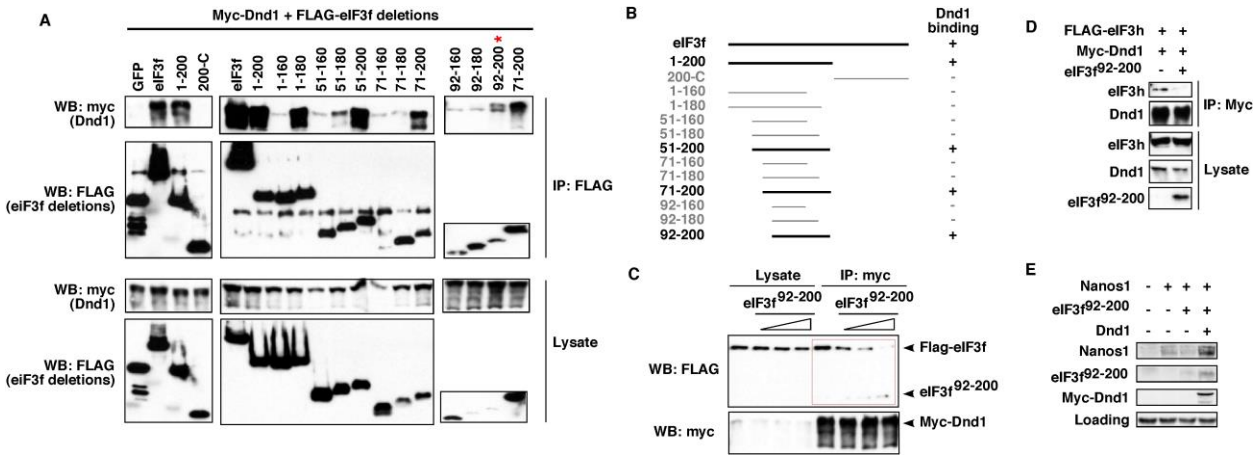

Figure 6. Interaction between Dnd1 and eIF3f is critical for *nanos1* translation. (A) FLAG-tagged eIF3f deletions were transfected into HEK293T cells along with myc-Dnd1. Lysates were immunoprecipitated with anti-FLAG antibody and analyzed by Western blot. **(B)** Schematic summarizing experiments shown in (A). "+" for Dnd1 binding; "-" lack of Dnd1 binding. **(C)** Myc-Dnd1 and FLAG-eIF3f were transfected into HEK293T cells with increasing amounts of eIF3f$^{92\text{-}200}$. Cell lysates were immunoprecipitated with an anti-myc antibody and analyzed by Western blot. **(D)** Myc-Dnd1 and FLAG-eIF3h were transfected into HEK293T cells in the presence or absence of eIF3f$^{92\text{-}200}$. Cell lysates were immunoprecipitated with an anti-myc antibody and analyzed by Western blot. Experiments were repeated for three times. **(E)** *nanos1* RNA was injected into fertilized eggs alone or with *eIF3f*$^{92\text{-}200}$, or with *eIF3f*$^{92\text{-}200}$ and *myc-dnd1* RNAs. At stage 11, Nanos1 protein was immunoprecipitated and analyzed by Western blot. Non-specific band served as a loading control. The experiment was performed two times.

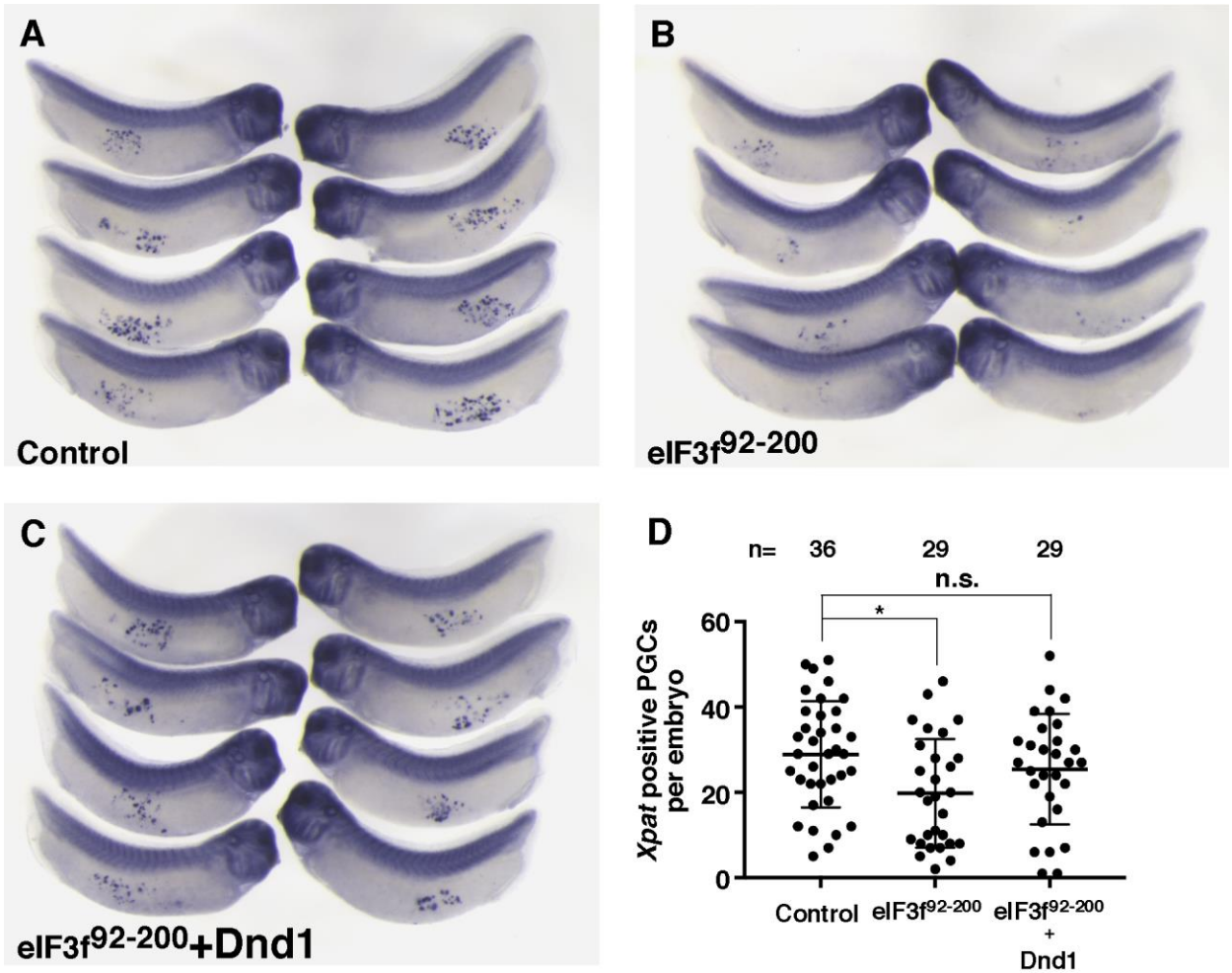

Figure 7. Interfering with the interaction between Dnd1 and eIF3f disrupts PGC development. (A-C) *In situ* hybridization of stage 33 embryos showing *Xpat*-expressing *PGCs* in uninjected controls **(A)**, *eIF3f*$^{92\text{-}200}$ injected **(B),** and *eIF3f*$^{92\text{-}200}$ + *dnd1* injected **(C)** embryos. Experiments were repeated for three times. **(D)** Quantification of results shown in F-H. Two-tailed *t*-test was performed. *p<0.05. n.s., nonsignificant.

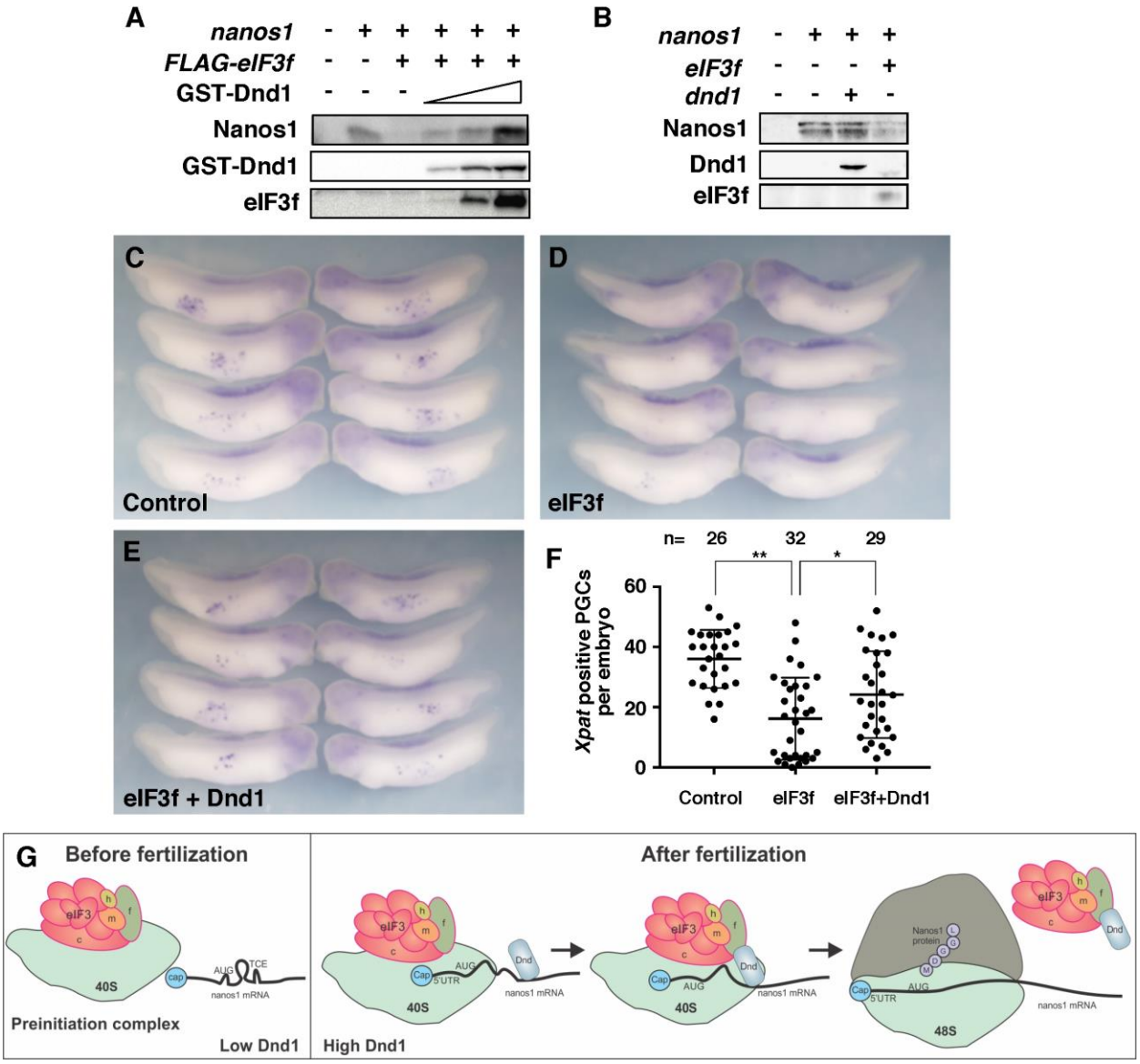

Figure 8. Dnd1 relieves the inhibitory effect of eIF3f on *nanos1* translation and PGC development. (A) *nanos1* (4 ng) was translated alone or with FLAG-eIF3f (2 ng) in wheat germ extracts with enhanced translational efficiency (Promega WG+). Nanos1 protein was detected by Western blot. eIF3f inhibited *nanos1* translation. Addition of recombinant Dnd1 protein relieved the repressive activity of eIF3f in a dose dependent manner. The experiment was repeated for

three times. **(B)** eIF3f represses *nanos1* translation *in vivo*. *nanos1* RNA was injected into fertilized eggs alone, or together with *eIF3f* or *dnd1* RNA. At stage 11, Nanos1 protein was immunoprecipitated and analyzed by Western blot. Experiments were performed twice. **(C-E)** *In situ* hybridization of stage 33 embryos showing PGCs by *Xpat staining* in uninjected controls **(C)**, *eIF3f* injected **(D),** and *eIF3f* + *dnd1* injected **(E)** embryos. Experiments were repeated three times. **(F)** Quantification of results shown in C-E. Two-tailed *t*-test was performed. *$p<0.05$, **$p<0.01$. **(G)** Working model of Dnd1 function in regulating *nanos1* translation. Before fertilization, very little Dnd1 protein is present. Translation of *nanos1* RNA is blocked by TCE, a secondary structure within the ORF that prevents the preinitiation complex (PIC) from scanning and initiating translation. After fertilization, Dnd1 protein accumulates within the germ plasm and there binds to *nanos1* RNA, altering the TCE structure. The PIC can now scan the *nanos1* RNA. Meanwhile, Dnd1 binds with the eIF3 complex through the interaction with subunit eIF3f. This interaction blocks the repressive activity of eIF3f and promotes the translation of *nanos1* RNA. The eIF3-Dnd1 complex is released from the 40S ribosomal subunit as translation proceeds.

Supplemental Figures

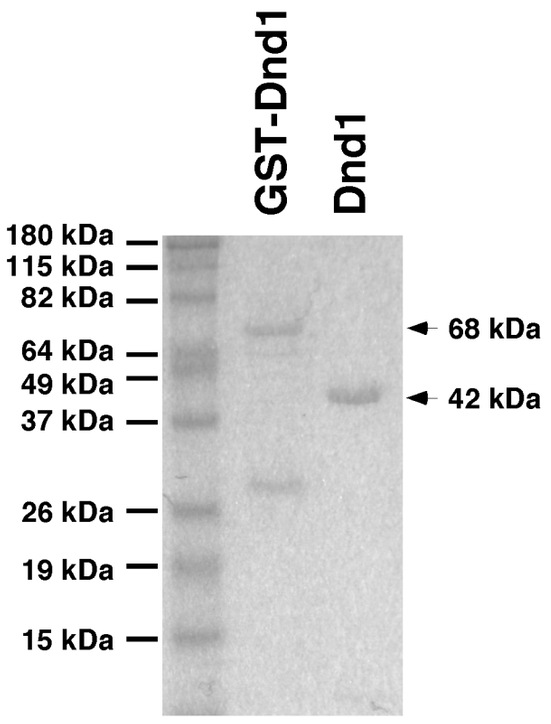

Figure S1. Coomassie blue staining showing purified GST-Dnd1 and Dnd1.

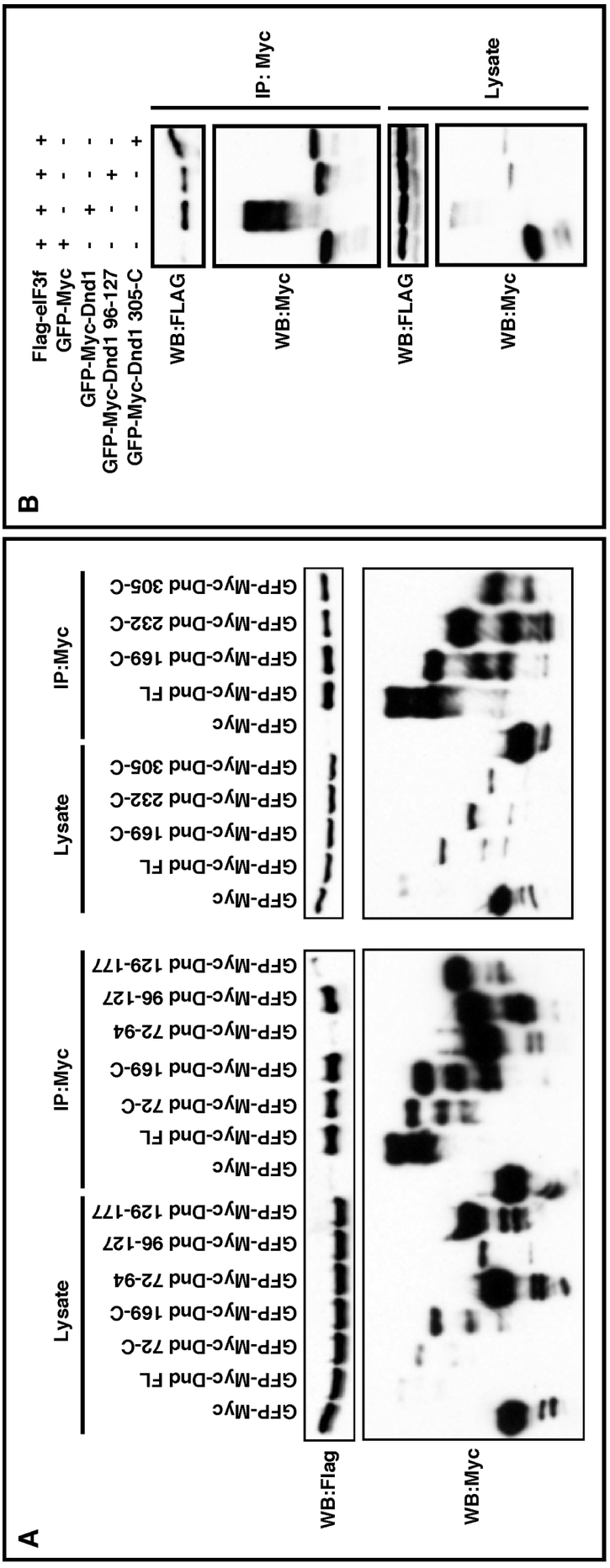

Figure S2. Mapping the eIF3f-binding domain of Dnd1. Because some Dnd1 deletion constructs are poorly expressed, we fused Dnd1 and deletions to GFP-Myc. These constructs were transfected into HEK293T cells together with FLAG-eIF3f. Lysates were immunoprecipitated with anti-Myc antibody and analyzed by Western blot. **(B)** CoIP to confirm that eIF3f interacts with Dnd1$^{96\text{-}127}$ and Dnd1$^{305\text{-}C}$.

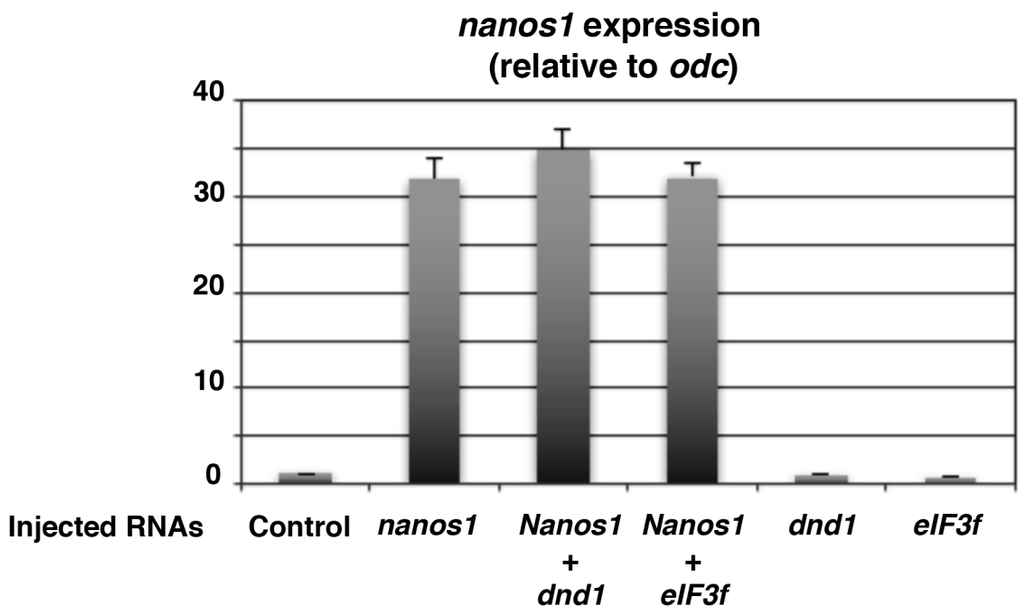

Figure S3. Overexpression of eIF3f has no effect on the stability of endogenous and overexpressed *nanos1* mRNAs. Fertilized eggs were injected vegetally with *nanos1, dnd1, eIF3f, nanos1 + dnd1, or nanos1 + eIF3f*. At the late blastula stage, embryos were harvested for RT-PCR analysis. The expression of *nanos1* was normalized to that of *odc*.

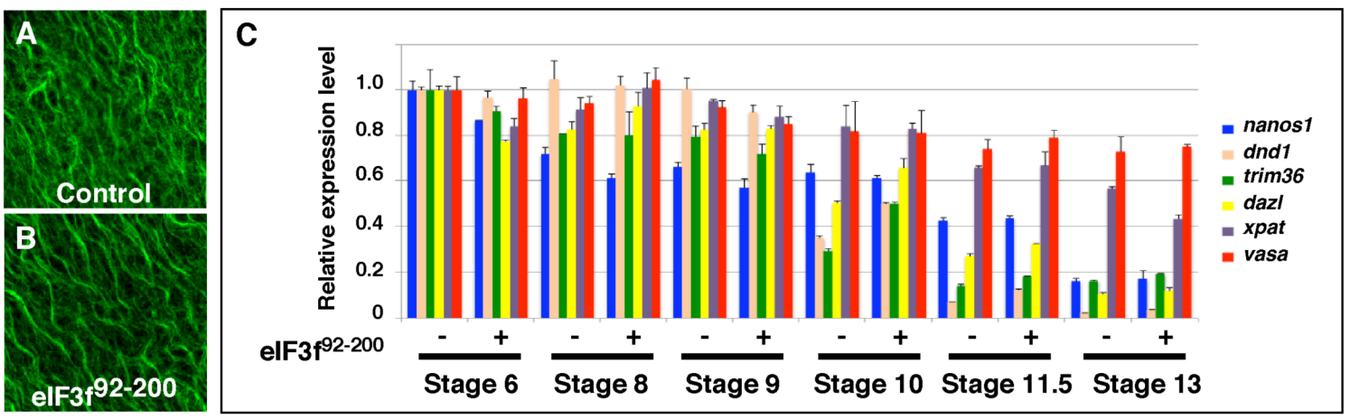

Figure S4. Overexpression of eIF3f$^{92\text{-}200}$ has no effect on formation of the vegetal cortical microtubule arrays during cortical rotation and degradation of germline specific RNAs during gastrulation. (A) and **(B)** Confocal images showing formation of microtubule arrays in the vegetal cortex in artificially activated eggs. Control (**A**) and eIF3f$^{92\text{-}200}$ (4 ng) overexpressed oocytes (**B**) were treated with progesterone to induce maturation, pricked with a glass needle after GVBD, harvested at 55 minutes post egg activation, and stained with an anti-Tubulin antibody. (**C**) Real-time PCR results show the expression of *nanos1*, *dnd1*, *trim36*, *dazl*, *Xpat*, and *vasa* in control and eIF3f$^{92\text{-}200}$ overexpressed embryos.

Supplemental Figures

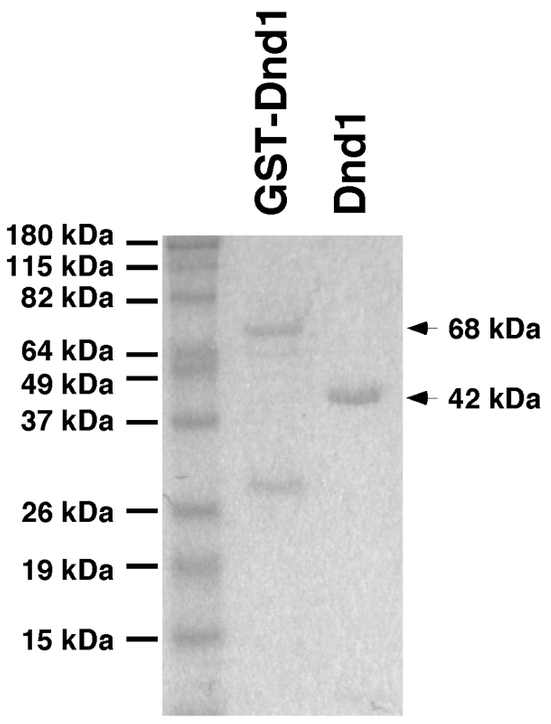

Figure S1. Coomassie blue staining showing purified GST-Dnd1 and Dnd1.

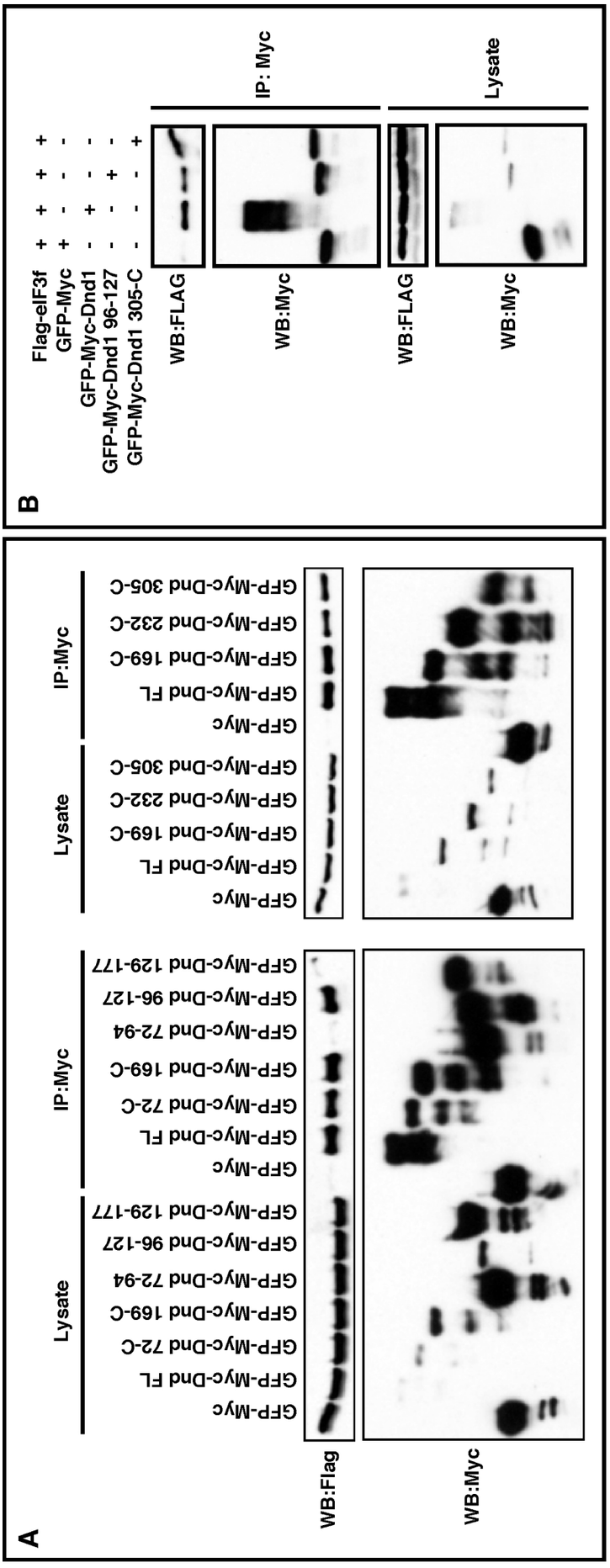

Figure S2. Mapping the eIF3f-binding domain of Dnd1. Because some Dnd1 deletion constructs are poorly expressed, we fused Dnd1 and deletions to GFP-Myc. These constructs were transfected into HEK293T cells together with FLAG-eIF3f. Lysates were immunoprecipitated with anti-Myc antibody and analyzed by Western blot. **(B)** CoIP to confirm that eIF3f interacts with Dnd1$^{96\text{-}127}$ and Dnd1$^{305\text{-}C}$.

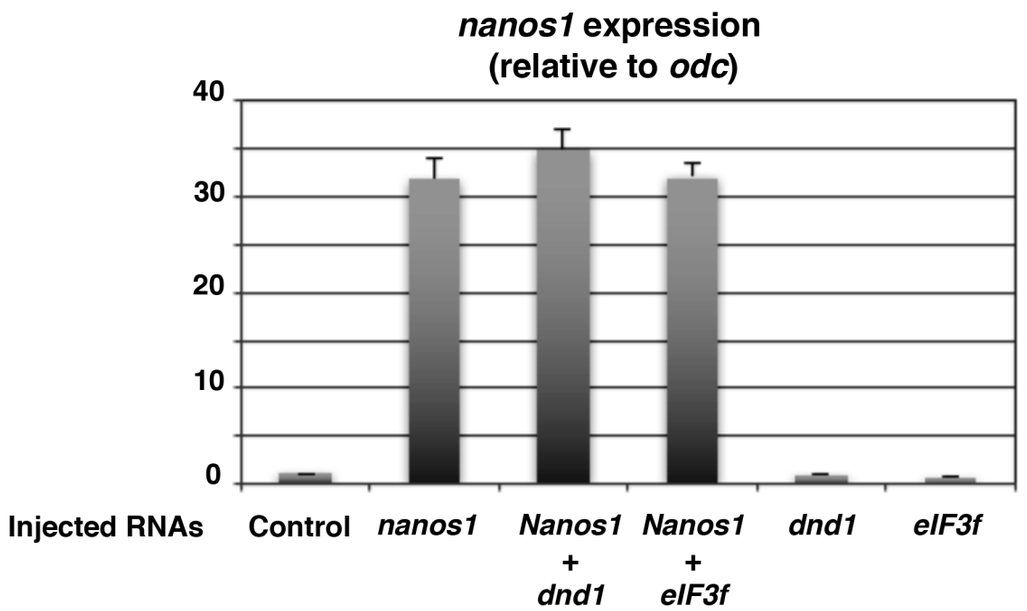

Figure S3. Overexpression of eIF3f has no effect on the stability of endogenous and overexpressed *nanos1* mRNAs. Fertilized eggs were injected vegetally with *nanos1, dnd1, eIF3f, nanos1 + dnd1, or nanos1 + eIF3f*. At the late blastula stage, embryos were harvested for RT-PCR analysis. The expression of *nanos1* was normalized to that of *odc*.

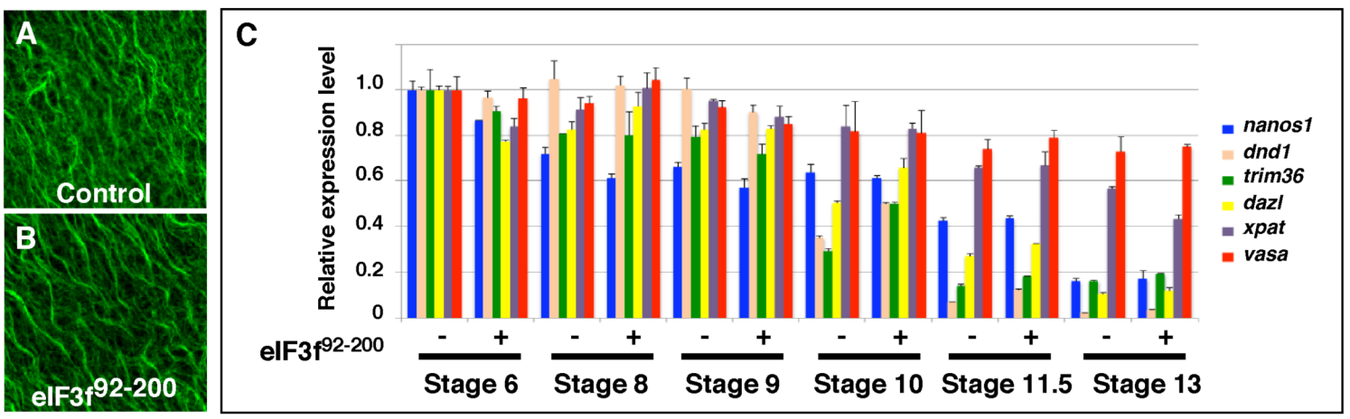

Figure S4. Overexpression of eIF3f$^{92\text{-}200}$ has no effect on formation of the vegetal cortical microtubule arrays during cortical rotation and degradation of germline specific RNAs during gastrulation. (A) and **(B)** Confocal images showing formation of microtubule arrays in the vegetal cortex in artificially activated eggs. Control (**A**) and eIF3f$^{92\text{-}200}$ (4 ng) overexpressed oocytes (**B**) were treated with progesterone to induce maturation, pricked with a glass needle after GVBD, harvested at 55 minutes post egg activation, and stained with an anti-Tubulin antibody. (**C**) Real-time PCR results show the expression of *nanos1*, *dnd1*, *trim36*, *dazl*, *Xpat*, and *vasa* in control and eIF3f$^{92\text{-}200}$ overexpressed embryos.